Adıyaman University Journal of Science
https://dergipark.org.tr/en/pub/adyujsci
DergiPark AKADEMİK
ISSN 2147-1630
e-ISSN 2146-586X

A Comparative Study of DFT/B3LYP/6-31G(d,p), RM062X/6-31G(d,p), B3LYP/6-311++G(d,p) and HSEH1PBE/6-31G(d,p) Methods Applied to Molecular Geometry and Electronic properties of C_s-$C_{60}Cl_6$ Molecule

Ebru KARAKAŞ SARIKAYA[1,*], Ömer DERELİ[2], Semiha BAHÇELİ[3]

[1]*Necmettin Erbakan of University, Engineering Faculty, Department of Basic Sciences, Konya, Türkiye*
ebrukarakas_84@hotmail.com, ORCID: 0000-0003-2149-9341
[2]*Necmettin Erbakan of University, Faculty of A. K. Education, Department of Physics, Konya, Türkiye*
odereli@erbakan.edu.tr, ORCID: 0000-0002-9031-8092
[3]*Emeritus Professor of Atomic and Molecular Physics, 06000, Ankara, Türkiye*
sbahceli@thk.edu.tr, ORCID: 0000-0002-5614-325X

Received: 16.05.2021 **Accepted:** 06.12.2021 **Published:** 31.12.2021

Abstract

In this study, four different levels, B3LYP/6-31G(d,p), RM062X/6-31G(d,p), B3LYP/6-311++G(d,p) and HSEH1PBE/6-31G(d,p) of the DFT quantum chemical calculation method have been applied to the molecular structure of the C_s-$C_{60}Cl_6$ molecule as a halogenated fullerene. Additionally, the molecular structure of pure C_{60} fullerene was presented as complementary and supportive work. Furthermore, the simulated FT-IR, Raman and UV-Vis (in cyclohexane solvent) spectra, HOMO-LUMO analysis, the molecular electrostatic potential (MEP) map, the ^{13}C NMR chemical shift values in both gas phase and tetrachloromethane with deuterated chloroform solvent and the thermodynamics properties at the mentioned levels of the C_s-$C_{60}Cl_6$ molecule were reported. Fullerene has many physical and electrochemical properties, which can be utilized in several medical fields. Especially, it can fit inside the hydrophobic cavity of HIV proteases, restricting the get into substrates to the catalytic site of the enzyme. Hence, it is utilizable as an antioxidant and radical scavenger.

* Corresponding Author DOI: 10.37094/adyujsci.938050

Keywords: Fullerenes; C_s-$C_{60}Cl_6$; DFT; HOMO-LUMO analysis; The ^{13}C NMR chemical shifts; MEP.

C_s-$C_{60}Cl_6$ Molekülünün Moleküler Geometri ve Elektronik Özelliklerine Uygulanan Metot ve Baz Seti, DFT/B3LYP/6-31G(d,p), RM062X/6-31G(d,p), B3LYP/6-311++ G(d,p) ve HSEH1PBE/6-31G(d,p), Yöntemlerinin Karşılaştırmalı İncelemesi

Öz

Bu çalışmada, DFT kuantum kimyasal hesaplama yönteminin, B3LYP/6-31G(d,p), RM062X/6-31G(d,p), B3LYP/6-311++G(d,p) ve HSEH1PBE/6-31G(d,p) olmak üzere dört farklı düzeyinde, halojenleşmiş bir fulleren olan C_s-$C_{60}Cl_6$ molekülünün moleküler yapısına uygulanmıştır. Ek olarak, saf C_{60} fullerenin molekül yapısı, tamamlayıcı ve destekleyici bir çalışma olarak sunulmuştur. Ayrıca, simüle edilmiş FT-IR, Raman ve UV-Vis (sikloheksan çözücüsünde) spektrumları, HOMO-LUMO analizi, moleküler elektrostatik potansiyel (MEP) haritası, döteryumlanmış kloroform çözücü ile hem gaz fazında hem de tetraklorometanda ^{13}C NMR kimyasal kayma değerleri ve C_s-$C_{60}Cl_6$ molekülünün belirtilen düzeylerdeki termodinamik özellikleri rapor edilmiştir. Fuleren, çeşitli tıbbi alanlarda kullanılabilecek birçok fiziksel ve elektrokimyasal özelliğe sahiptir. Özellikle, HIV proteazlarının hidrofobik boşluğunun içine sığabilir ve substratlara enzimin katalitik bölgesine girmesini kısıtlayabilir. Bu nedenle, bir antioksidan ve radikal temizleyici olarak kullanılabilir.

Anahtar Kelimeler: Fulleren; C_s-$C_{60}Cl_6$; DFT; HOMO-LUMO analizi; ^{13}C NMR kimyasal kayma; MEP.

1. Introduction

As the best example for the monotype molecules, the fullerene or Buckminster fullerene C_{60}, which derives its name from the geodesic dome designed by the architect Buckminster Fuller, is any of a series of hollow carbon molecules [1-4]. Over 40 years after its discovery, the fullerenes still attract the attention of many researchers in various scientific and technological fields such as nanotechnology, material science, medicine, chemistry, and physics [5-10]. Although the fullerene C_{60} is the most popularly applied in a large range of fields, the other fullerenes with a different number of carbon atoms were also discovered. Within this framework, the sizes of hollow carbon polyhedra called fullerenes vary from C_{20} to lattices of more than 400 carbon atoms [11-12].

Furthermore, the derivatives of the various fullerene complexes with heavy metals were also found the interesting applications in medicinal chemistry, material science, and nanotechnology [13-17].

On the other hand, it is well-known that halogen bonding occurred in a substance with a halogen atom provides a nucleophilic region which plays a crucial role in pharmacology, materials sciences and biology [18]. In this context, the halogenated fullerenes have also been investigated intensively during the last two decades and demonstrate encouraging characteristics toward material science utilizations since they are flexible predecessors for the synthesis of diverse intricate derivatives. In this framework, the chloro fullerenes are very useful for the halogen derivatives with optical and biomedical properties [19-22]. Likewise, sizable completion has been accomplished in the development and structural specification related to fullerene bromides [19] and fluorides [23]. Regardless of countless statements on chlorination of C_{60} via distinct reagents, solely two characteristic compounds have been seal off density functional theory (DFT) for fullerene derivatives has been broadly experienced in describe their structure and molecular properties [24-27]. In this context, the use of the B3LYP level with the 6-31G* basis set of the theory can be mentioned for applicability to large molecules [28].

DFT is used for calculating molecular geometry parameters of compounds, spectroscopic properties such as Raman, ^{1}H and ^{13}C NMR chemical shift values and thermodynamic characteristics, UV-Vis spectra, IR, electronic features like HOMO, MEP, and LUMO of the compounds [29]. Take into consideration, the satisfactory electronic correlation influences and selecting capable basis sets in this technique, the trustworthy vibrational frequencies and optimized geometric coefficients of molecules be able to foresee [30-33]. At the beginning of the 1990s in DFT, the Becke-3-Lee Yang Parr (B3LYP) hybrid approach and the Becke's three parameters incorporating Perdew and Wang's 1991 (B3PW91) approach are labeled first-generation methods, and the Heyd−Scuseria−Ernzerhof hybrid combined with Perdew, Burke, and Ernzerhof's exchange and correlation functions (HSEH1PBE) approach, which is also mentioned as the HSE06 approach, is a second-generation method [33-37].

Our study is settled on research carried out by Kuvychko et al. [21] in where the Infrared and Raman spectra of C_s-$C_{60}Cl_6$ were extensively investigated by both experimental studies and the vibrational frequency computations toward the PBE/6-31G* grade of the principles. However, the molecular structure and electronic properties of the C_s-$C_{60}Cl_6$ molecule were not studied properly in the mentioned work. Therefore, even if it is an absence of experimental information considering DFT calculations are a forceful quantum chemical instrument for the identification

of the electronic frame related to molecules, we found it worth focusing on investigating the molecular frame and electronic features of C_s-$C_{60}Cl_6$ compounds in detailed data [38, 39].

In this framework, the present work reports the results of the quantum chemical calculations of the optimized molecular construction, the FT-IR, UV-Vis (in cyclohexane solvent) and FT-Raman by using the B3LYP/6-31G(d,p), RM062X/6-31G(d,p), B3LYP/6-311++G(d,p), and HSEH1PBE/6-31G(d,p) levels of the theory [34,40,41]. In this article, abbreviations will be used BS-1 for B3LYP/6-31G(d,p), BS-2 for RM062X/6-31G(d,p), BS-3 for B3LYP/6-311++G(d,p), BS-4 for HSEH1PBE/6-31G(d,p), respectively. Furthermore, the NMR chemical shifts (^{1}H and ^{13}C) both in tetrachloromethane solutions and in the gas-phase; the UV spectrum in cyclohexane (the upper limit electronic suction wavelengths given that λ_{max}); LUMO-HOMO energy spaces and thermodynamics characteristics of the C_s-$C_{60}Cl_6$ molecule are presented.

2. Materials and Methods

2.1. Computational details

In this study, optimization calculations in the ground state were made in the Gaussian 09W [42] program for all conformations. The output files were contemplated via Gauss View software. [43]. Also, calculations were performed by Dell Rack server. The structural properties, which is electronic properties and molecular geometry of the C_s-$C_{60}Cl_6$ fullerene molecule, were estimate at the BS-1, BS-2, BS-3 and BS-4 levels of the DFT. However, the simulated FT-Raman and FT-IR vibrational spectra of the C_s-$C_{60}Cl_6$ molecule were presented by computing at the mentioned levels [34, 40, 41]. Furthermore, the optimized structure of the C_{60} fullerene was calculated with only at the BS-1 method.

Nevertheless, the stable structure of the C_s-$C_{60}Cl_6$ fullerene molecule was initially obtained with the BS-3 method by way of CPCM (the conductor-like polarizable continuum technique). After that, NMR values were determined using GIAO (the gauge-including atomic orbital) method attribute to optimization at the mentioned levels in tetrachloromethane with deuterated chloroform and in the gas phase (ϵ= (2.24 and 4.8)) [38, 45]. The UV-Vis spectra (in ethanol and in the gas phase) were acquired utilizing the time-dependent DFT (TD-DFT) theory at the BS-1, BS-2 and BS-3 levels [46, 47]. Furthermore, the FMO and MEP maps that figure out the title compound were performed through the BS-1, BS-2, BS-3 and BS-4 levels of the theory additionally, their 3D plots were confirmed at the mentioned level.

3. Results and Discussion

3.1. Molecular structures

The stable structures of the fullerene C_{60} molecule at the BS-1 and the C_s-$C_{60}Cl_6$ fullerene molecule at the BS-3 levels, respectively, and their atom numbers are exhibited in Fig. 1.

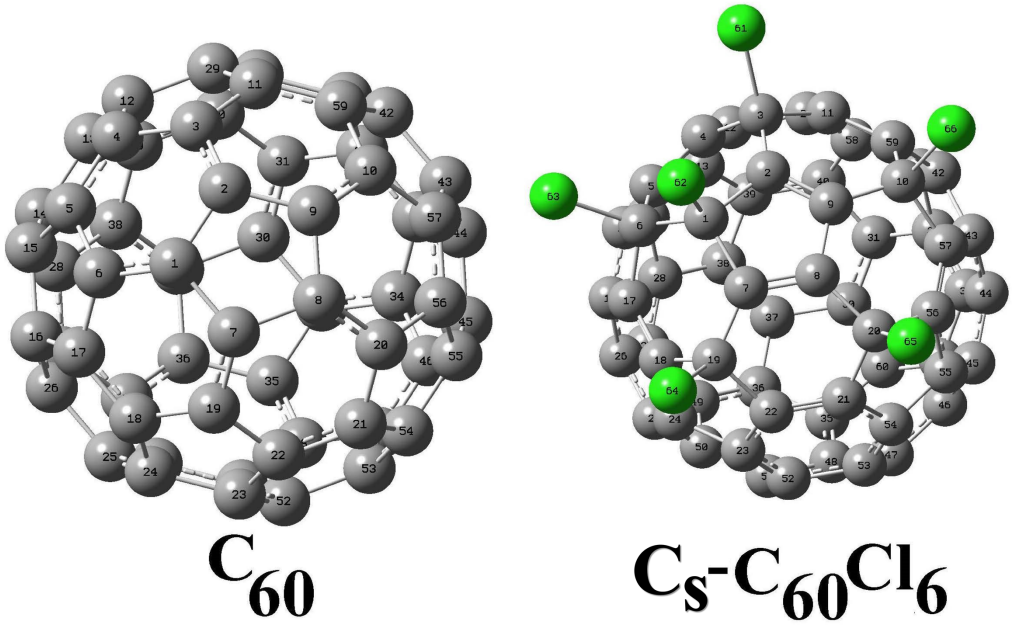

Figure 1: The stable optimized molecular structures of the C_{60} fullerene at the BS-1 level on the left and the C_s-$C_{60}Cl_6$ molecule at the BS-3 level on the right with their atom numberings

Table 1: The calculated most stable state energy values of C_{60} and C_s-$C_{60}Cl_6$ fullerenes

	Method/Basis set	*E* (Hartree)	Dip. Mom. (D)
C_{60}	**(BS-1)**	-2286.174135	0.000000
C_s-$C_{60}Cl_6$	**(BS-1)**	-5047.325711	6.476442
C_s-$C_{60}Cl_6$	**(BS-2)**	-5046.447915	5.267343
C_s-$C_{60}Cl_6$	**(BS-3)**	-5044.200344	5.527418
C_s-$C_{60}Cl_6$	**(BS-4)**	-5047.944625	5.238593

Furthermore, the calculated energy values of the fullerene C_{60} and the C_s-$C_{60}Cl_6$ compound for their most stable states are summed up in Table 1. Nonetheless, the stable geometry parameters of the C_{60} fullerene calculated with the BS-1 method are stated in Table S1 as the supplementary material. Similarly, the optimized molecular geometry parameters calculated at the BS-1, BS-2, BS-3 and BS-4 levels of the C_s-$C_{60}Cl_6$ compound are given in Table S2.

As far as we know, the researchers have not been yet performed X-ray spectroscopy work on the C_s-$C_{60}Cl_6$ sample. However, the chlorination with ICl produces the C_s-$C_{60}Cl_6$ compound which is isostructural with $Cl_{60}Br_6$ [48-49]. For this reason, we used some crystallographic values

of the $Cl_{60}Br_6$ compound [48] in order to compare with the bond lengths calculated withal the BS-1 of C_s-$C_{60}Cl_6$ fullerene. In this context, the C_s-$C_{60}Cl_6$ molecular has a non-crystallographic C_s symmetry, a monoclinic crystal system, and a P21/c space group [48-49]. Therefore, the experimental values of the C-C(Cl) single bonds, the C-Cl bond lengths, and the remaining C-C bonds in the central pentagons of the C_s-$C_{60}Cl_6$ fullerene should be averaged 1.96 Å, 1.53 Å and 1.45 Å while the remaining inter pentagonal C-C bonds should be averaged 1.38 Å [49-50]. According to our calculations which are shown in Table S2, the C-Cl bond lengths in the pentagons can be averaged 1.85 Å at the BS-1 and BS-3 methods, 1.81 Å at the BS-3 method and 1.82 Å at the BS-4 method. The dissimilarity among the experimental C-Br and theoretical C-Cl bond lengths which is about 0.11 Å can be attributed to the effect of chlorine halogen atom on the bond with C atom as less electronegative than Br atoms [50]. Similarly, the C1-C2, C1-C7 and C8-C9 single bond lengths in the pentagon of the C_s-$C_{60}Cl_6$ fullerene were calculated as 1.54 Å at the BS-1, BS-2 and BS-3 levels, and as 1.53 Å at the BS-4 level which is excellent correspondence with the experimental results [48]. Likewise, the C7=C8 and C2=C29 double bonds in the pentagon were reckoned as 1. 35Å and 1.34 Å at the BS-1 level and also worked out BS-2, BS-3 and BS-4 levels, respectively, for both double bonds which are also in perfect match with the experimental values [51], while the C1-C6 and C8-C20 single bonds in inter pentagon were found as 1.58 Å at the BS-1 and BS-3 levels, and as 1. 57 Å at the BS-2 and BS-4 levels.

Moreover, by considering Fig. 1 and Table S1 for C_{60} fullerene the calculated C-C single bonds at the BS-1 level can be averaged almost as 1.45 Å and the double C=C bonds can be also averaged as 1.39 Å. These calculated data are in excellent correspondence including the values in the literature [52]. Therefore, by considering the given results we can state that the chlorination of C_{60} fullerene exhibits a significant distortion on the fullerene.

Furthermore, as seen in Table S2, we can declare that the dihedral angles and bond of the C_s-$C_{60}Cl_6$ molecule computed at the mentioned four different levels can be formed a database for the studies about the halogenated fullerenes in the future.

3.2. Vibrational frequencies

While we pointed out in the section introduction, the experimental and theoretical determined at the PBE/TZ2P level Infrared and Raman vibrational frequency values of the C_s-$C_{60}Cl_6$ molecule were given in the work which was verified by Kuvychko et al. [21]. Furthermore, the experimental infrared vibrational frequencies [53] and the assignments of the infrared and Raman vibrational band modes were verified in the early studies [19, 21, 54]. For this reason, we

presented here, only the simulated IR and Raman vibrational spectra of the C_s-$C_{60}Cl_6$ molecule at the BS-1, BS-2, BS-3 and BS-4 levels are shown in Figs. 2 and 3, respectively.

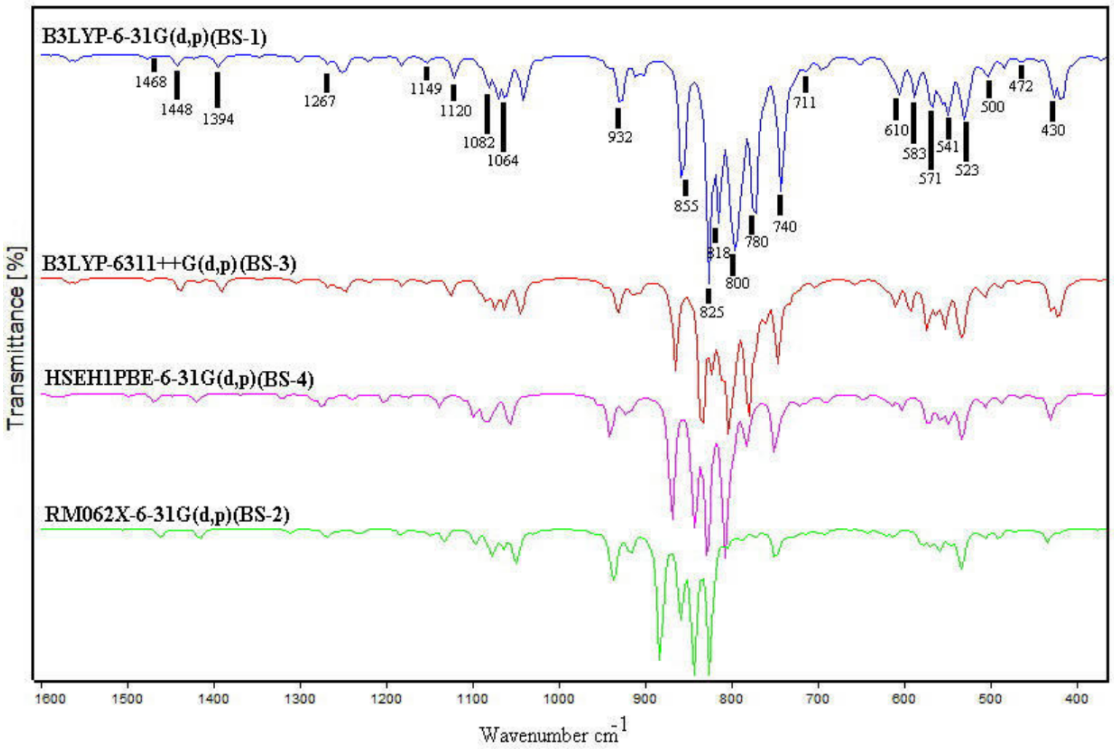

Figure 2: The simulated IR spectra at the BS-1, BS-2, BS-3 and BS-4 levels for the C_s-$C_{60}Cl_6$ molecule

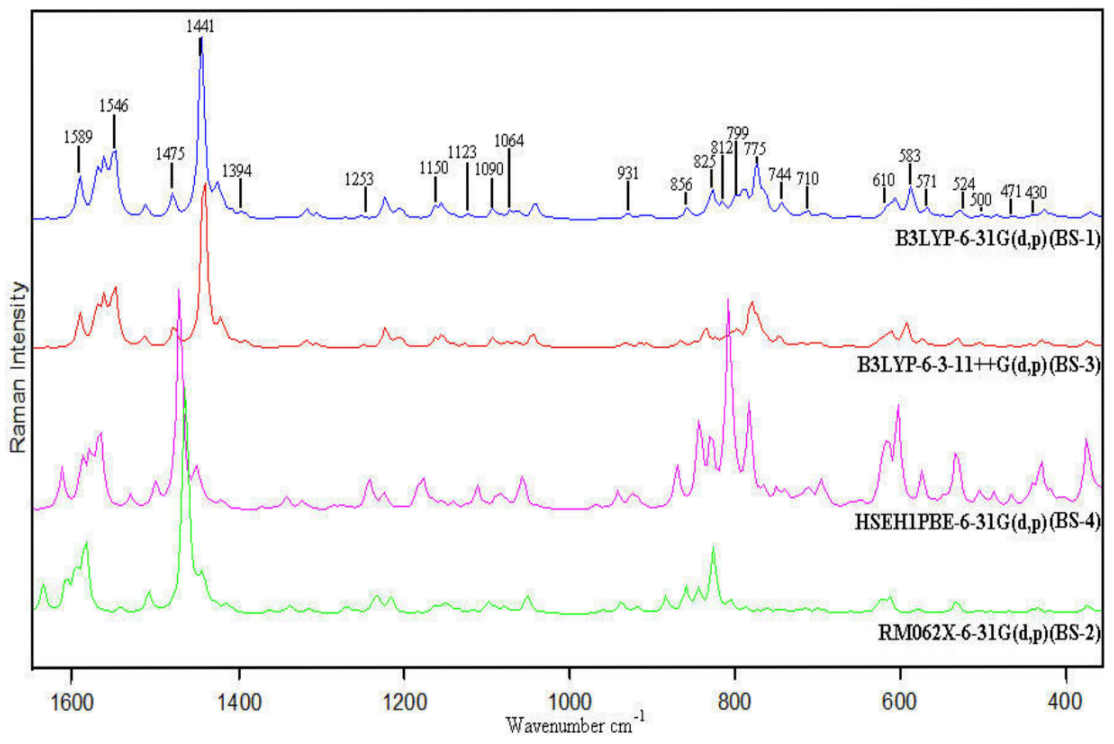

Figure 3: The simulated Raman spectra at the BS-1, BS-2, BS-3 and BS-4 levels for the C_s-$C_{60}Cl_6$ molecule

As seen in Figs. 2 and 3, the both IR and Raman vibrational frequency values computed with the BS-1 method are in excellent correspondence including the experimental values given in [53] while the values computed at the remaining levels exhibit very slightly shifts from all vibrational bands.

3.3. NMR analysis

It is well-known that nuclear magnetic resonance (NMR) is a crucial instrument to grasp the magnetic properties which satisfy accurately the prediction of molecular structures and the isotropic chemical shifts that allow identifying the relative ionic species [53-54]. The obtained results from our calculations are given in Table S4 for both in tetrachloromethane with deuterated chloroform solvent and gas phase of C_s-$C_{60}Cl_6$ molecule. NMR spectra of the C_s-$C_{60}Cl_6$ molecule at the BS-1, BS-2, BS-3 and BS-4 levels are shown in Fig. 4.

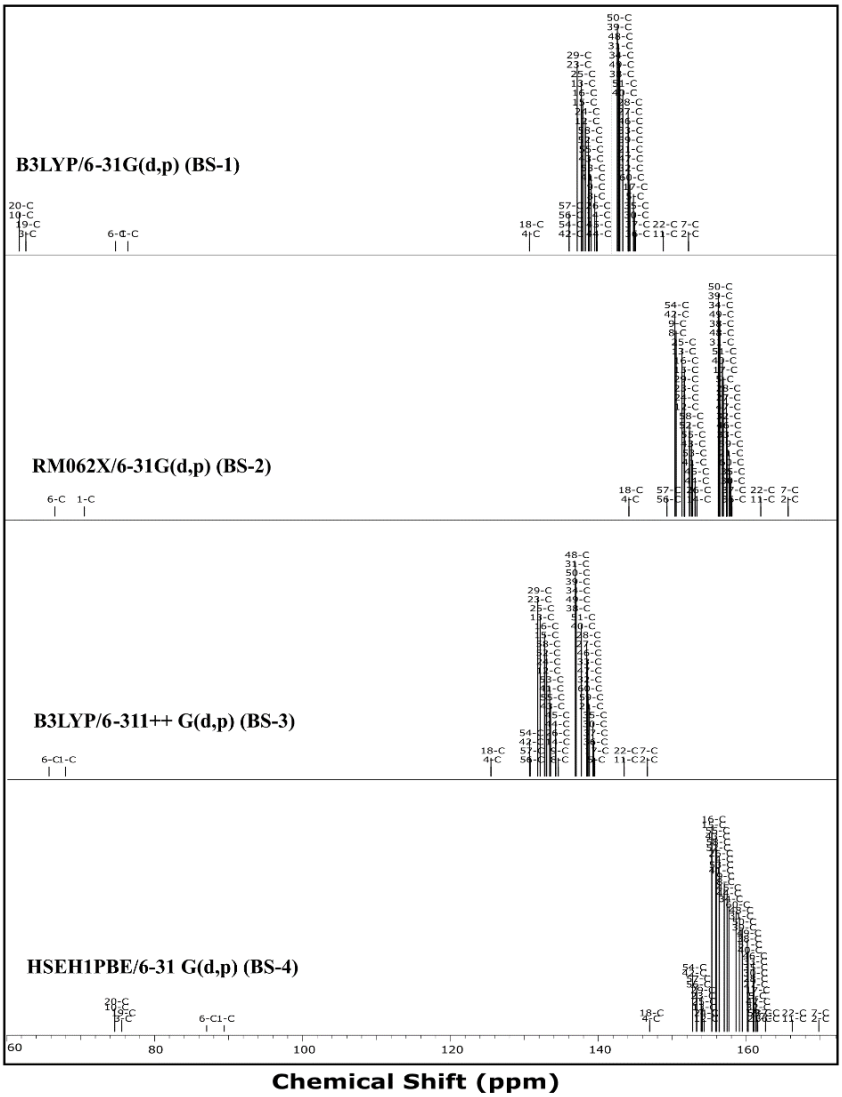

Figure 4: The simulated NMR spectra at the BS-1, BS-2, BS-3 and BS-4 levels for the C_s-$C_{60}Cl_6$ molecule

By considering Table S3 the experimental/calculated values in tetrachloromethane with deuterated chloroform solvent at the BS-1, BS-2, BS-3 and BS-4 levels for C1, C3 and C20 which are connected to the chlorine atoms with high electronegativity of the C_s-$C_{60}Cl_6$ molecule were found at 69.4 ppm/ 76.5, 70.8, 67.8, 89.4 ppm, 55.4 ppm/63.1, 55.2, 54.8, 75.5 ppm and 54.9 ppm/ 62.2, 54.5, 53,9, 74,6 ppm, respectively [48]. Therefore, we can state that the experimental and computed with the BS-4 method for C^{13} NMR features of the cited carbon atoms are in good agreement. Otherwise, the highest C^{13} NMR chemical shift values as experimentally/ theoretically in the mentioned chemical solution were found in the regions 152.8-146.9 ppm/ 169.8- 161.3 ppm at the BS-3 level as seen in Table S3.

3.4. UV-Visible spectroscopy and HOMO-LUMO analysis

The simulated at the BS-1, BS-2 and BS-4 levels of the theorem UV-Vis spectra in the cyclohexane solvent and gas-phase of the C_s-$C_{60}Cl_6$ molecule are handed over in Fig. 5. Furthermore, the calculated λ_{max} worth, f oscillator strengths (vacuum/cyclohexane) and also excitation energies are presented in Table 2. By considering Table 2 and Fig. 5, the resemblance between the experimental and computed λ_{max} values at the cited levels demonstrates that the nearest to experimental values valid for the values calculated with BS-2 method [53].

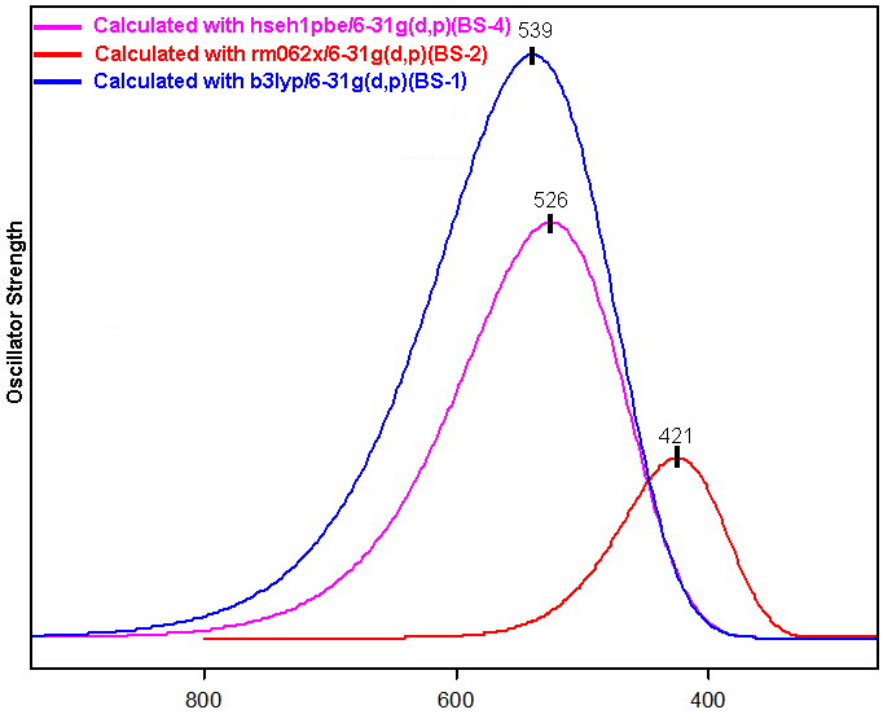

Figure 5: The simulated UV-Vis spectra in the cyclohexane solvent and gas phase at the BS-1, BS-2 and BS-4 levels for the C_s-$C_{60}Cl_6$ molecule

Therefore, the recorded electronic absorption bands at 380 nm, 280 nm and 257 nm in the cyclohexane solvent can correspond to the computed wavelengths at 427.26/428.22 nm, 421.42/421.43 nm and 418.25/418.30 nm in vacuum/cyclohexane at the BS-2 level, respectively which are attributed to the transitions n→ π* and π→ π*, respectively [53, 55].

However, the deviation among the experimental and computed λ_{max} worth for the transition n→ π* is 48.22 nm while this difference values become 141.43 nm and 161.3 nm for the transitions π→ π* which are highly large. For this reason, the UV-Vis spectroscopy for fullerenes derivatives was found as an unreliable method in the past [56]. These differences in the λ_{max} worth computed at the BS-1 and BS-4 levels of the theory for the C_s-$C_{60}Cl_6$ molecule were found larger than those worth worked out at the BS-2 level. The calculated data can see by looking at Table 2 and Fig. 5.

Table 2: The calculated at the BS-1, BS-2 and BS-4 levels of the theory UV-Vis parameters in the cyclohexane solvent and gas phase of the C_s-$C_{60}Cl_6$ molecule

Experimental*	**(BS-1)**	**(BS-2)**	**(BS-3)**
λ_{max} (nm)	λ_{max} (nm)	λ_{max} (nm)	λ_{max} (nm)
(in cyclohexane)	(vacuum/ cyclohexane)	(vacuum/ cyclohexane)	(vacuum/ cyclohexane)
386	545.40/ 553.69	427.26/ 428.22	532.67/ 537.61
280	534.55/ 539.45	421.42/ 421.43	524.40/ 526.80
257	518.72/ 518.52	418.25/ 418.30	505.28/ 512.82
211	Excitation energies (eV)	Excitation energies (eV)	Excitation energies (eV)
	(vacuum/ cyclohexane)	(vacuum/ cyclohexane)	(vacuum/ cyclohexane)
	2.2733/ 2.2392	2.9018/ 2.8953	2.3276/ 2.3062
	2.3194/ 2.2984	2.9420/ 2.9420	2.3643/ 2.3535
	2.3902/ 2.3911	2.9643/ 2.9640	2.4538/ 2.4177
	f (oscillator strengths)	f (oscillator strengths)	f (oscillator strengths)
	(vacuum/ cyclohexane)	(vacuum/ cyclohexane)	(vacuum/ cyclohexane)
	0.0002/ 0.0006	0.0001/ 0.0002	0.0001/ 0.0003
	0.0000/ 0.0000	0.0000/ 0.0000	0.0000/ 0.0001
	0.0002/ 0.0004	0.0001/ 0.0001	0.0004/ 0.0003

Taken from ref. [53].

On the other hand, the lowest occupied and highest unoccupied molecular orbitals (LUMO and HOMO) are also called the frontier molecular orbitals (or FMOs) and are played an important role in chemical reaction [57, 58].

The formed energy space among LUMO and HOMO molecular orbitals, which is a crucial parameter, indicates the molecular chemical stability. Furthermore, molecular properties such as electronegativity, kinetic stability, chemical reactivity, polarizability, softness, and chemical hardness, and aromaticity can find out via utilizing this energy space [57, 59].

Figure 6 shows the 3D plots of LUMO-HOMO molecular orbitals for the C_s-$C_{60}Cl_6$ molecule obtained at the BS-1, BS-2, BS-3 and BS-4 levels in the result of our calculation.

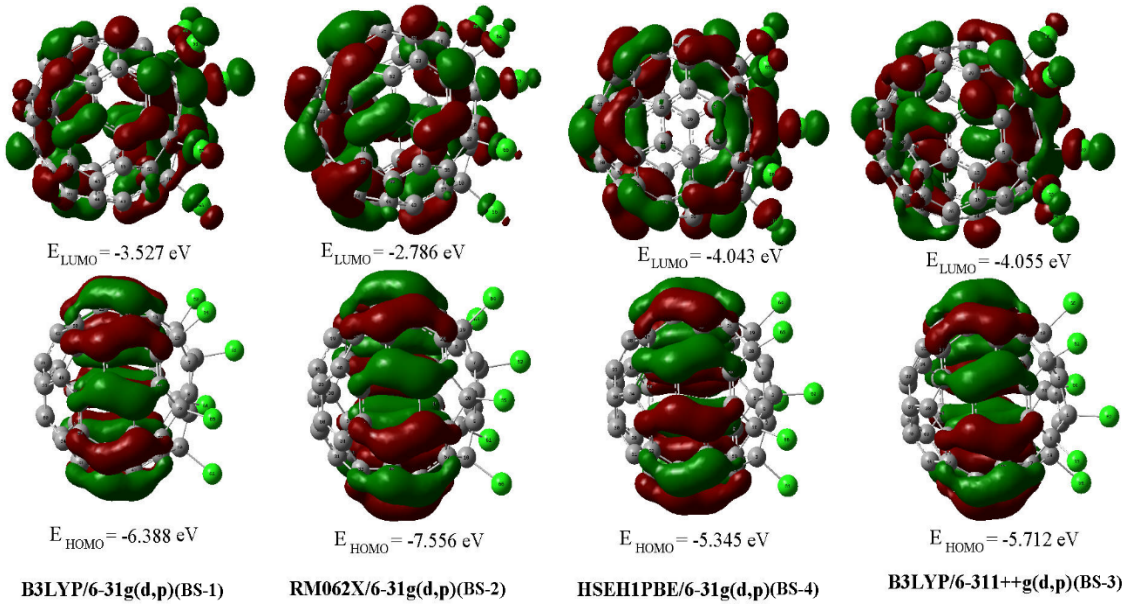

Figure 6: The 3D plots of HOMO-LUMO of the C_s-$C_{60}Cl_6$ molecule obtained at the BS-1, BS-2, BS-3 and BS-4 levels

Table 3: Some molecular properties of C_s-$C_{60}Cl_6$ molecules

Method/Basis set	**BS-1**	**BS-2**	**BS-3**	**BS-4**	
Electronic Energy (EE)	-5047.325711	-5046.447915	-5044.200344	-5047.944625	Hartree
Zero-point Energy Correction	0.383416	0.391142	0.389969	0.382543	Hartree
Thermal Correction to Energy	0.414375	0.421606	0.420520	0.413441	Hartree
Thermal Correction to Enthalpy	0.415319	0.422550	0.421464	0.414385	Hartree
Thermal Correction to Free Energy	0.328937	0.336738	0.335767	0.328075	Hartree
EE + Zero-point Energy	-5046.942295	-5046.056772	-5043.810375	-5047.562082	Hartree
EE + Thermal Energy Correction	-5046.911337	-5046.026309	-5043.779824	-5047.531184	Hartree
EE + Thermal Enthalpy Correction	-5046.910392	-5046.025365	-5043.778880	-5047.530240	Hartree
EE + Thermal Free Energy Correction	-5046.996775	-5046.111176	-5043.864577	-5047.616550	Hartree
E (Thermal)	260.024	264.562	263.880	259.438	kcal/mol
Heat Capacity (C_v)	146.280	143.598	144.230	146.103	cal/mol-K
Entropy (S)	181.806	180.606	180.365	181.654	cal/mol-K

By using the calculated energy gap values between the HOMO–LUMO levels given in Fig. 6, some molecular properties of the C_s-$C_{60}Cl_6$ compound were indexed in Table 3 [60]. Therefore, the calculated energy gap value at the BS-2 level was found as 4.77 eV as seen in Table 3. However, this value is not in excellent correspondence including the calculated energy value at the BS-2 level of about 3 eV for the transition n→ π* as can be understood from Table 2. However, these differences are even greater in the other three levels. These results support the view that the UV-Vis technique is not reliable for the fullerene derivatives [56].

3.5. The molecular electrostatic potential (MEP)

So as to understand the molecular affects in structure, the molecular electrostatic potential (MEP) is well-known as a significant instrument. Also, MEP mapping is a valuable tool to study molecular properties, like electronegativity, chemical reactivity, dipole moments, and partial charges of molecules. On the other hand, the MEP has also described as the affect energy among a unit positive test charge and the charge distribution of the molecule [61,62]. Generally, the electrostatic potentials on surfaces are shown in different colors. Consequently, the blue and red painted sections illustrate the zones of positive and negative electrostatic potential while green colored sections demonstrate the zones with zero potential. The negative zones of molecular electrostatic potential are associated with electrophilic reactivity and also the positive zone are associated with nucleophilic reactivity.

In our calculations, we present the 3D plots of the MEP for the C_s-$C_{60}Cl_6$ molecule by using the optimized molecular structures at the BS-1, BS-2, BS-3 and BS-4 levels in Fig. 7.

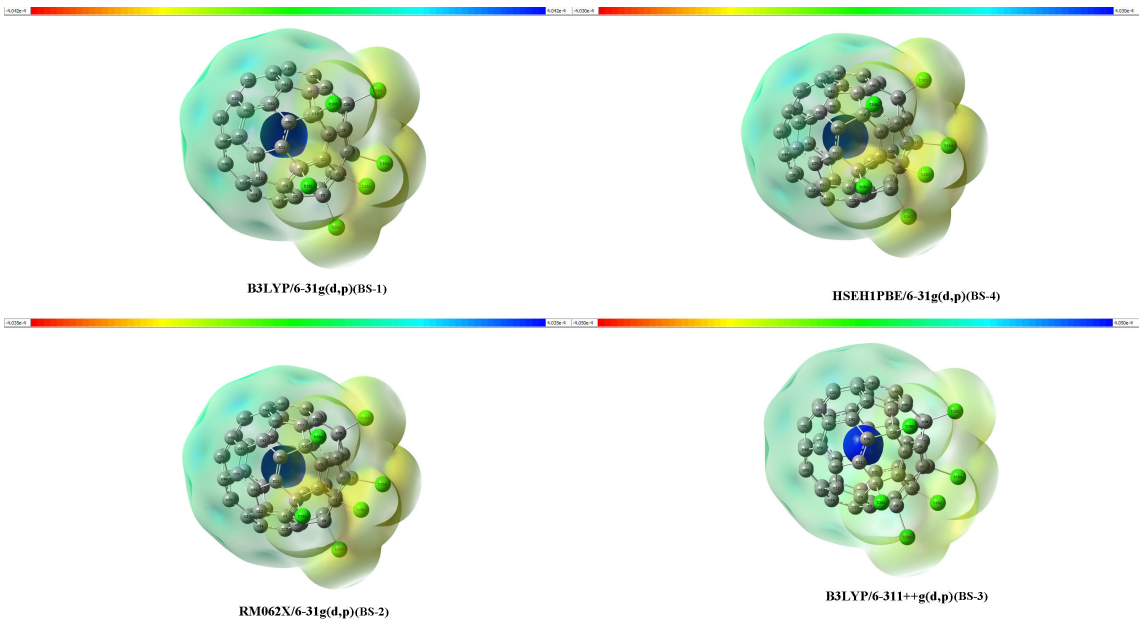

Figure 7: Molecular electrostatic potential (MEP) surface of the C_s-$C_{60}Cl_6$ molecule obtained at the BS-1, BS-2, BS-3 and BS-4 levels.

By considering Fig. 7, the negative regions (with red color or seems to be yellow here) of the MEP plane are confined on the Cl atoms in the C_s-$C_{60}Cl_6$ molecule while the dark blue and blue sites are localized on the carbon atoms that are in the core of the title compound. On the other hand, the green regions are confined to the surroundings of the fullerene cage.

3.6. Thermodynamic parameters

The total energy of molecular structure is the sum of its vibrational, rotational, electronic and translational energies ($E = E_v + E_r + E_e + E_t$). Furthermore, the thermodynamic parameters like rotational constants (GHz), entropy, S, heat capacity, C_v, thermal energy, E, zero-point vibration energy, ZPVE, dipole moment can be calculated by using DFT computational methods [63-65]. In the gas phase, the computed thermodynamic parameters of the C_s-$C_{60}Cl_6$ molecule at the BS-1, BS-2, BS-3 and BS-4 levels are donated in Table 4.

According to Table 4, the minimum energy of the C_s-$C_{60}Cl_6$ was found as -5047.944625 Hartree DFT calculations at the BS-3 method. Meanwhile sum calculated thermal energies were realized to be 260.024, 264.552, 263.880, and 259.438 kcal/mol at the BS-1, BS-2, BS-3 and BS-4 levels, respectively.

Table 4: The calculated thermodynamic parameters (in gas phase) of C_s-$C_{60}Cl_6$ molecule

Method/Basis set	**BS-1**	**BS-2**	**BS-3**	**BS-4**	
Electronic Energy (EE)	-5047.325711	-5046.447915	-5047.944625	-5044.200344	Hartree
Zero-point Energy Correction	0.383416	0.391142	0.382543	0.389969	Hartree
Thermal Correction to Energy	0.414375	0.421606	0.413441	0.420520	Hartree
Thermal Correction to Enthalpy	0.415319	0.422550	0.414385	0.421464	Hartree
Thermal Correction to Free Energy	0.328937	0.336738	0.328075	0.335767	Hartree
EE + Zero-point Energy	-5046.942295	-5046.056772	-5047.562082	-5043.810375	Hartree
EE + Thermal Energy Correction	-5046.911337	-5046.026309	-5047.531184	-5043.779824	Hartree
EE + Thermal Enthalpy Correction	-5046.910392	-5046.025365	-5047.530240	-5043.778880	Hartree
EE + Thermal Free Energy Correction	-5046.996775	-5046.111176	-5047.616550	-5043.864577	Hartree
E (Thermal)	260.024	264.562	259.438	263.880	kcal/mol
Heat Capacity (C_v)	146.280	143.598	146.103	144.230	cal/mol-K
Entropy (S)	181.806	180.606	181.654	180.365	cal/mol-K

Taken from ref. [48].

4. Conclusion

In the current study, the examination of the stable structure of the C_s-$C_{60}Cl_6$ molecule at the BS-1, BS-2, BS-3 and BS-4 levels of the theory and the stable molecular structure of C_{60} fullerene at the BS-1 level was presented as a supportive work. Similarly, the simulated Raman and Infrared spectra of the C_s-$C_{60}Cl_6$ at the noticed level are in excellent correspondence including the experimental data. The ^{13}C NMR chemical shift values of the C_s-$C_{60}Cl_6$ compound in tetrachloromethane with deuterated chloroform solution and gas-phase were verified at the noticed levels.

The computed chemical shift values in tetrachloromethane with deuterated chloroform solvent at the BS-4 level of the carbon atoms which are connected to the Cl halogen atoms of the C_s-$C_{60}Cl_6$ molecule are in excellent correspondence including the experimental data. The simulated UV-Vis spectra of the C_s-$C_{60}Cl_6$ molecule in the cyclohexane solvent and gas-phase

were computed at the BS-1, BS-2 and BS-4. Furthermore, the MEP and HOMO–LUMO analyses and thermodynamic parameters of the C_s-$C_{60}Cl_6$ molecule at the mentioned levels were also presented.

References

[1] Kroto, H.W., Heath, J.R., O'Brien, S.C., Curl, R.F. Smalley, R.E., *C_{60}:Buckminsterfullerene,* Nature, 318(6042), 162-163, 1985.

[2] Ward, J., ed., *The artifacts of R. buckminster fuller: A comprehensive collection of his designs and drawings in four volumes*, New York: Garland, 1984.

[3] Krätschmer, W., Fostiropoulos, K., Huffman, D.R., *The infrared and ultraviolet absorption spectra of laboratory-produced carbon dust: evidence for the presence of the C_{60} molecule*, Chemical Physics Letters, 170(2-3), 167-170, 1990.

[4] Kroto, H.W., Allaf, A.W., Balm, S.P., *C_{60}:Buckminsterfullerene*, Chemical Reviews, 91(6), 1213-1235, 1991.

[5] Lin, T., Zhang, W.D., Huang, J., He, C.A., *DFT study of the amination of fullerenes and carbon nanotubes: reactivity and curvature,* The Journal of Physical Chemistry B, 109(28), 13755-13760, 2005.

[6] Yang, C.C., Shen, J.Y., *Well-defined sensing property of ZnO: Al relative humidity sensor with selected buffer layer,* Vacuum, 118, 118-124, 2015.

[7] Nalwa, H.S., ed. *Handbook of advanced electronic and photonic materials and devices*, ten-volume set, Academic Press, 1 ed., United States, 2000.

[8] Omacrsawa, E., *Perspectives of fullerene nanotechnology,* Kluwer Academic Publisher, Dordrecht-Boston-London, 2002.

[9] Bianco A., Da Ros T., Langa. F., Nierengarten J.F., *Biological applications of fullerenes, in fullerenes principles and applications,* Royal Society of Chemistry, 10, 301-328, 2008.

[10] Hudhomme P., Cousseau, J., Langa. F., Nierengarten J.F., *Plastic solar cells using fullerene derivatives in the photoactive layer, in fullerenes principles and applications,* Royal Society of Chemistry, 8, 221-265, 2008.

[11] So, H.Y., Wilkins, C.L., *First observation of carbon aggregate ions >C_{600}^+ by laser desorption Fourier transform mass spectrometry,* The Journal of Physical Chemistry, 93(4), 1184-1187, 1989.

[12] Rubin, Y., Kahr, M., Knobler, C.B., Diederich, F., Wilkins, C.L., *The higher oxides of carbon $C_{8n}O_{2n}$ (n= 3-5): synthesis, characterization, and X-ray crystal structure. Formation of cyclo [n] carbon ions C_n^+ (n= 18, 24), C_n^- (n= 18, 24, 30), and higher carbon ions including C_{60}^+ in laser desorption Fourier transform mass spectrometric experiments,* Journal of the American Chemical Society, 113(2), 495-500, 1991.

[13] Makurin, Y.N., Sofronov, A.A., Gusev, A.I., Ivanovsky, A.L., *Electronic structure and chemical stabilization of C_{28} fullerene*, Chemical Physics, 270(2), 293-308, 2001.

[14] Lin, M., Chiu, Y.N., Lai, S.T., Xiao, J., Fu, M., *Theoretical study of metallofullerenes M@C_{32},* Journal of Molecular Structure: Theochem, 422(1-3), 57-67, 1998.

[15] Guo, T., Smalley, R.E., Scuseria, G.E., *Ab initio theoretical predictions of C_{28}, $C_{28}H_4$, $C_{28}F_4$, (Ti@C_{28})H_4, and M@C_{28} (M= Mg, Al, Si, S, Ca, Sc, Ti, Ge, Zr, and Sn),* The Journal of Chemical Physics, 99(1), 352-359, 1993.

[16] Kadish, K.M., Ruoff, R.S., *Fullerenes: chemistry, physics, and technology*, John Wiley & Sons, Newyork, 2000.

[17] Prinzbach, H., Weiler, A., Landenberger, P., Wahl, F., Wörth, J., Scott, L.T., Issendorff, B.V., *Gas-phase production and photoelectron spectroscopy of the smallest fullerene, C_{20},* Nature, 407(6800), 60-63, 2000.

[18] Priimagi, A., Cavallo, G., Metrangolo, P., Resnati, G., *The halogen bond in the design of functional supramolecular materials: recent advances,* Accounts of Chemical Research, 46(11), 2686-2695, 2013.

[19] Popov A.A., Senyavin V.M., and Granovsky A.A., *Vibrational spectra of chloro- and bromofullerenes,* Fullerenes, Nanotubes, And Carbon Nanostructures*,* Marcel Dekker, 12, 305–310, 2004.

[20] Troshin, P.A., Lyubovskaya, R.N., Ioffe, I.N., Shustova, N.B., Kemnitz, E., Troyanov, S.I., *Synthesis and structure of the highly chlorinated [60]Fullerene $C_{60}Cl_{30}$ with a drum-shaped carbon cage,* Angewandte Chemie International Edition, 44(2), 234-237, 2005.

[21] Kuvychko, I.V., Streletskii, A.V., Popov, A.A., Kotsiris, S.G., Drewello, T., Strauss, S.H., Boltalina, O.V., *Seven-minute synthesis of pure Cs-$C_{60}Cl_6$ from [60] Fullerene and iodine monochloride: First IR, Raman, and Mass spectra of 99 mol% $C_{60}Cl_6$,* Chemistry A European Journal, 11(18), 5426-5436, 2005.

[22] Yan, Q.B., Zheng, Q.R., Su, G., *Theoretical study on the structures, properties and spectroscopies of fullerene derivatives $C_{66}X_4$ (X= H, F, Cl),* Carbon, 45(9), 1821-1827, 2007.

[23] Troyanov, S.I., Boltalina, O.V., Kouvytchko, I.V., Troshin, P.A., Kemnitz, E., Hitchcock, P.B., Taylor, R., *Molecular and crystal structure of the adducts of $C_{60}F_{18}$ with aromatic hydrocarbons,* Fullerenes, Nanotubes And Carbon Nanostructures, 10(3), 243-259, 2002.

[24] Adjizian, J.J., Vlandas, A., Rio, J., Charlier, J.C., Ewels, C.P., *Ab initio infrared vibrational modes for neutral and charged small fullerenes (C_{20}, C_{24}, C_{26}, C_{28}, C_{30} and C_{60}),* Philosophical Transactions Of The Royal Society A: Mathematical, Physical And Engineering Sciences, 374(2076), 20150323, 2016.

[25] Yang, T., Zhao, X., Nagase, S., *Di-lanthanide encapsulated into large fullerene C_{100}: a DFT survey,* Physical Chemistry Chemical Physics, 13(11), 5034-5037, 2011.

[26] Carter, E.A., Rossky, P.J., *Computational and theoretical chemistry,* Accounts of Chemical Research, 39(2), 71-72, 2006.

[27] Bauernschmitt, R., Ahlrichs, R., Hennrich, F.H., Kappes, M.M., *Experiment versus time dependent density functional theory prediction of fullerene electronic absorption,* Journal of the American Chemical Society, 120(20), 5052-5059, 1998.

[28] Schettino, V., Pagliai, M., Cardini, G., *The infrared and Raman spectra of fullerene C_{70}. DFT calculations and correlation with C_{60}*, The Journal of Physical Chemistry A, 106(9), 1815-1823, 2002.

[29] Jensen, F. *Introduction to computational chemistry*, John Wiley & Sons, Newyork, 664p., 3 ed., 1974.

[30] Pulay, P., *Ab initio calculation of force constants and equilibrium geometries in polyatomic molecules: I. Theory,* Molecular Physics, 17(2), 197-204, 1969.

[31] Perdew, J.P., "*Electronic Structure of Solids", in Proceeding of the 21st Annual International Symposium,* p11, 1991.

[32] Perdew, J. P., Wang, Y., *Pair-distribution function and its coupling-constant average for the spin-polarized electron gas,* Physical Review B, 46(20), 12947, 1992.

[33] Becke, A.D., *A new mixing of Hartree–Fock and local density-functional theories,* The Journal of Chemical Physics, 98(2), 1372-1377, 1993.

[34] Lee, C., Yang, W., Parr, R.G., *Development of the Colle-Salvetti correlation-energy formula into a functional of the electron density*, Physical Review B, 37(2), 785, 1988.

[35] Burke, K., Perdew, J.P., Wang, Y., *Derivation of a Generalized Gradient Approximation: The PW_{91} Density Functional,* Electronic Density Functional Theory, Springer, Boston, MA., 81-111, 1998.

[36] Zhao, Y., Pu, J., Lynch, B. J., Truhlar, D.G., *Tests of second-generation and third-generation density functionals for thermochemical kinetics,* Physical Chemistry Chemical Physics, 6(4), 673-676, 2004.

[37] Heyd, J., Scuseria, G.E., Ernzerhof, M., *Hybrid functionals based on a screened Coulomb potential,* The Journal of Chemical Physics, 118(18), 8207-8215, 2006.

[38] Wolinski, K., Hinton, J.F., Pulay, P., *Efficient implementation of the gauge-independent atomic orbital method for NMR chemical shift calculations,* Journal of the American Chemical Society, 112(23), 8251-8260, 1990.

[39] Avcı, D., Dede, B., Bahceli, S., Varkal, D., *Spectroscopic and quantum chemical calculation study on 2–ethoxythiazole molecule,* Journal of Molecular Structure, 1138, 110-117, 2017.

[40] Heyd, J., Scuseria, G.E., Ernzerhof, M., *Hybrid functionals based on a screened Coulomb potential,* The Journal of Chemical Physics, 118(18), 8207-8215, 2003.

[41] Zhao, Y., Truhlar, D.G., *Comparative DFT study of van der Waals complexes: Rare-Gas Dimers, Alkaline-Earth Dimers, Zinc Dimer, And Zinc-Rare-Gas Dimers,* The Journal of Physical Chemistry A, 110(15), 5121-5129, 2006.

[42] Frisch, M.J., Trucks, G.W., Schlegel, H.B., Scuseria, G.E., Robb, M.A., Cheeseman, J.R., ... Fox, D.J., *Gaussian 09*, Gaussian, Inc., Wallingford CT, 2009.

[43] Dennington, R., Keith, T., Millam, J., *GaussView Version 5.* Semichem Inc., Shawnee Mission, Kans, 2009.

[44] Foresman, J.B., Frisch., E., *Exploring chemistry with electronic structure methods,* Gaussian Inc., Pittsburgh, Pa., USA, 1993.

[45] London, F. *Théorie quantique des courants interatomiques dans les combinaisons aromatiques*, Journal de Physique et le Radium, 8(10), 397-409, 1937.

[46] Bauernschmitt, R., Ahlrichs, R., *Treatment of electronic excitations within the adiabatic approximation of time dependent density functional theory,* Chemical Physics Letters, 256(4-5), 454-464, 1996.

[47] Jamorski, C., Casida, M.E., Salahub, D.R., *Dynamic polarizabilities and excitation spectra from a molecular implementation of time-dependent density-functional response theory: N_2 as a case study,* The Journal of Chemical Physics, 104(13), 5134-5147, 1996.

[48] Birkett, P.R., Hitchcock, P.B., Kroto, H.W., Taylor, R., Walton, D.R., *Preparation and characterization of $C_{60}Br_6$ and* $C_{60}Br_8$, Nature, 357(6378), 479-481, 1992.

[49] Birkett, P.R., Avent, A.G., Darwish, A.D., Kroto, H.W., Taylor, R., Walton, D.R., *Holey fullerenes! a bis-lactone derivative of [70 fullerene with an eleven-atom orifice,* Journal of the Chemical Society, Chemical Communications, 18, 1869-1870, 1995.

[50] Politzer, P., Murray, J.S., Clark, T., *Halogen bonding and other σ-hole interactions: a perspective*, Physical Chemistry Chemical Physics, 15(27), 11178-11189, 2013.

[51] Troyanov, S.I., Troshin, P.A., Boltalina, O.V., Kemnitz, E., *Bromination of [60]Fullerene. II. Crystal and molecular structure of [60]Fullerene bromides, $C_{60}Br_6$, $C_{60}Br_8$, and $C_{60}Br_{24}$,* Fullerenes, Nanotubes and Carbon Nanostructures, 11(1), 61-77, 2003.

[52] Fedurco, M., Olmstead, M.M., Fawcett, W.R., *Single-crystal X-ray structure of C_{60}•6$SbPh_3$. A well-ordered structure of C_{60} and a new fullerene solvent*, Inorganic Chemistry, 34(1), 390-392, 1995.

[53] Birkett, P.R., Avent, A.G., Darwish, A.D., Kroto, H.W., Taylor, R., Walton, D.R.M, *Preparation and ^{13}C NMR spectroscopic characterisation of $C_{60}Cl_6$,* Journal of the Chemical Society, Chemical Communications, 15, 1230-1232, 1993.

[54] Kuvychko, I.V., Streletskii, A.V., Shustova, N.B., Seppelt, K., Drewello, T., Popov, A.A., Boltalina, O.V., *Soluble Chlorofullerenes $C_{60}Cl_{2,4,6,8,10}$. Synthesis, purification, compositional analysis, stability, and experimental/theoretical structure elucidation, including the X-ray structure of C_1-$C_{60}Cl_{10}$,* Journal of the American Chemical Society, 132(18), 6443-6462, 2010.

[55] Süleymanoğlu, N., Ustabaş, R., Alpaslan, Y.B., Eyduran, F., İskeleli, N.O., *Experimental and theoretical investigation of the molecular and electronic structure of 3-ethoxy-4-isopropylaminocyclobut-3-ene-1,2-dione,* Spectrochimica Acta Part A: Molecular and Biomolecular Spectroscopy, 96, 35-41, 2012.

[56] Popov, A.A., Kareev, I.E., Shustova, N.B., Stukalin, E.B., Lebedkin, S.F., Seppelt, K., Dunsch, L., *Electrochemical, spectroscopic, and DFT study of $C_{60}(CF_3)_n$ frontier orbitals (n= 2−18): the link between double bonds in pentagons and reduction potentials,* Journal of the American Chemical Society, 129(37), 11551-11568, 2007.

[57] Pearson, R.G., *Absolute electronegativity and hardness correlated with molecular orbital theory,* Proceedings of the National Academy of Sciences, 83(22), 8440-8441, 1986.

[58] Lee, C.K., Kim, Y.H. *Spectroscopic studies of conjugated uracil derivatives*, Bulletin of the Korean Chemical Society, 12(2), 207-210, 1991.

[59] Fukui, K., *Role of frontier orbitals in chemical reactions*, Science, 218(4574), 747-754, 1982.

[60] Chtita, S., Ghamali, M., Larif, M., Adad, A., Hmammouchi, R., Bouachrine, M., Lakhlifi, T., *Prediction of biological activity of imidazo [1,2-a] pyrazine derivatives by combining DFT and QSAR results,* International Journal of Innovative Research in Science, Engineering and Technology, 2(11), 7951-7962, 2013.

[61] Murray, J.S., Sen K. eds., *Molecular electrostatic potentials concepts and applications,* Elsevier Science BV, Amsterdam, The Netherlands, 1996.

[62] Pîrnău, A., Chiş, V., Oniga, O., Leopold, N., Szabo, L., Baias, M.,nCozar, O., *Vibrational and DFT study of 5-(3-pyridyl-methylidene)-thiazolidine-2-thione-4-one,* Vibrational spectroscopy, 48(2), 289-296, 2008.

[63] Sarıkaya, E.K., Bahçeli, S., Varkal, D., Dereli, Ö., *FT-IR, micro-Raman and UV–vis spectroscopic and quantum chemical calculation studies on the 6-chloro-4-hydroxy-3-phenyl pyridazine compound,* Journal of Molecular Structure, 1141, 44-52, 2017.

[64] Yilmaz, M., Aydin, B., Dogan, O., Dereli, O., *Molecular structure and spectral investigations of 3,5-Di-tert-butyl-o-benzoquinone,* Journal of Molecular Structure, 1128, 345-354, 2017.

[65] Fankam, J.B., Ejuh, G.W., Tchangnwa N.F., Ndjaka, J.M.B., *Theoretical investigation of the molecular structure, vibrational spectra, thermodynamic and nonlinear optical properties of 4,5-dibromo-2,7dinitro-fluorescein,* Optical and Quantum Electronics, 52, 1-23, 2020.

SUPPLEMENTARY INFORMATION FILE

Adıyaman University Journal of Science
https://dergipark.org.tr/en/pub/adyujsci
DergiPark AKADEMİK
ISSN 2147-1630
e-ISSN 2146-586X

A Comparative Study of DFT/B3LYP/6-31G(d,p), RM062X/6-31G(d,p), B3LYP/6-311++G(d,p) and HSEH1PBE/6-31G(d,p) Methods Applied to Molecular Geometry and Electronic properties of C_s-$C_{60}Cl_6$ Molecule

Ebru KARAKAŞ SARIKAYA[1,*], Ömer DERELİ[2], Semiha BAHÇELİ[3]

[1]*Necmettin Erbakan of University, Engineering Faculty, Department of Basic Sciences, Konya, Türkiye*
ebrukarakas_84@hotmail.com, ORCID: 0000-0003-2149-9341
[2]*Necmettin Erbakan of University, Faculty of A. K. Education, Department of Physics, Konya, Türkiye*
odereli@erbakan.edu.tr, ORCID: 0000-0002-9031-8092
[3]*Emeritus Professor of Atomic and Molecular Physics, 06000, Ankara, Türkiye*
sbahceli@thk.edu.tr, ORCID: 0000-0002-5614-325X

* Corresponding Author

DOI: 10.37094/adyujsci.938050

Table S1. The calculated geometric parameters at the B3LYP/6-31G(d,p) level of C_{60} fullerene molecule. Bond lengths in Angstrom (Å) and angles in Degrees (°).

Bond Lenght		***Bond Angles***		***Bond Angles***		***Dihedral Angles***		***Dihedral Angles***	
C(60)-C(34)	1.395	C(35)-C(60)-C(30)	107.996	C(12)-C(4)-C(3)	107.993	C(30)-C(60)-C(34)-	138.191	C(13)-C(39)-C(38)-	0.001
C(60)-C(30)	1.453	C(35)-C(60)-C(34)	119.983	C(2)-C(3)-C(11)	119.998	C(30)-C(60)-C(34)-	0.002	C(39)-C(38)-C(37)-	0.007
C(60)-C(35)	1.453	C(30)-C(60)-C(34)	120.004	C(2)-C(3)-C(4)	120.007	C(35)-C(60)-C(34)-	0.029	C(39)-C(38)-C(37)-	138.211
C(59)-C(42)	1.453	C(10)-C(59)-C(11)	120.002	C(11)-C(3)-C(4)	108.017	C(35)-C(60)-C(34)-	-138.160	C(28)-C(38)-C(37)-	-138.181
C(59)-C(11)	1.396	C(10)-C(59)-C(42)	108.008	C(3)-C(2)-C(9)	120.006	C(34)-C(60)-C(30)-	-142.614	C(28)-C(38)-C(37)-	0.023
C(59)-C(10)	1.453	C(11)-C(59)-C(42)	120.006	C(3)-C(2)-C(1)	120.008	C(34)-C(60)-C(30)-	0.028	C(39)-C(38)-C(28)-	-0.007
C(58)-C(41)	1.453	C(29)-C(58)-C(40)	119.991	C(9)-C(2)-C(1)	108.010	C(35)-C(60)-C(30)-	-0.021	C(39)-C(38)-C(28)-	-142.663
C(58)-C(40)	1.453	C(29)-C(58)-C(41)	120.002	C(6)-C(1)-C(7)	120.004	C(35)-C(60)-C(30)-	142.621	C(37)-C(38)-C(28)-	142.612
C(58)-C(29)	1.396	C(40)-C(58)-C(41)	108.003	C(6)-C(1)-C(2)	119.983	C(34)-C(60)-C(35)-	142.633	C(37)-C(38)-C(28)-	-0.044
C(57)-C(43)	1.453	C(56)-C(57)-C(43)	119.996	C(7)-C(1)-C(2)	107.996	C(34)-C(60)-C(35)-	-0.024	C(38)-C(37)-C(30)-	142.630
C(57)-C(56)	1.396	C(56)-C(57)-C(10)	119.985	C(33)-C(34)-C(46)	108.001	C(30)-C(60)-C(35)-	0.031	C(38)-C(37)-C(30)-	-0.012
C(57)-C(10)	1.453	C(43)-C(57)-C(10)	108.002	C(33)-C(34)-C(60)	119.989	C(30)-C(60)-C(35)-	-142.626	C(36)-C(37)-C(30)-	0.004
C(56)-C(55)	1.453	C(20)-C(56)-C(55)	107.999	C(46)-C(34)-C(60)	120.009	C(11)-C(59)-C(42)-	-142.647	C(36)-C(37)-C(30)-	-142.638
C(56)-C(20)	1.453	C(20)-C(56)-C(57)	120.010	C(32)-C(33)-C(34)	120.004	C(11)-C(59)-C(42)-	-0.012	C(30)-C(37)-C(36)-	0.015
C(55)-C(45)	1.395	C(55)-C(56)-C(57)	120.013	C(32)-C(33)-C(44)	120.016	C(10)-C(59)-C(42)-	-0.004	C(30)-C(37)-C(36)-	142.627
C(55)-C(54)	1.453	C(45)-C(55)-C(56)	119.993	C(34)-C(33)-C(44)	108.011	C(10)-C(59)-C(42)-	142.632	C(38)-C(37)-C(36)-	-142.617
C(54)-C(53)	1.396	C(45)-C(55)-C(54)	120.019	C(33)-C(32)-C(41)	119.999	C(42)-C(59)-C(11)-	138.176	C(38)-C(37)-C(36)-	-0.005
C(54)-C(21)	1.453	C(56)-C(55)-C(54)	108.010	C(33)-C(32)-C(31)	120.013	C(42)-C(59)-C(11)-	0.019	C(49)-C(36)-C(35)-	-142.644
C(53)-C(47)	1.453	C(21)-C(54)-C(53)	120.009	C(41)-C(32)-C(31)	108.012	C(10)-C(59)-C(11)-	-0.039	C(49)-C(36)-C(35)-	0.014
C(53)-C(52)	1.453	C(21)-C(54)-C(55)	107.993	C(30)-C(31)-C(40)	119.988	C(10)-C(59)-C(11)-	-138.197	C(37)-C(36)-C(35)-	-0.028
C(52)-C(51)	1.453	C(53)-C(54)-C(55)	119.999	C(30)-C(31)-C(32)	119.979	C(42)-C(59)-C(10)-	-0.004	C(37)-C(36)-C(35)-	142.629
C(52)-C(23)	1.396	C(52)-C(53)-C(47)	107.991	C(40)-C(31)-C(32)	107.994	C(42)-C(59)-C(10)-	-142.623	C(60)-C(34)-C(33)-	142.657
C(51)-C(48)	1.453	C(52)-C(53)-C(54)	119.992	C(31)-C(30)-C(60)	120.011	C(11)-C(59)-C(10)-	142.642	C(60)-C(34)-C(33)-	-0.013
C(51)-C(50)	1.396	C(47)-C(53)-C(54)	119.979	C(31)-C(30)-C(37)	120.010	C(11)-C(59)-C(10)-	0.022	C(46)-C(34)-C(33)-	0.031
C(50)-C(49)	1.453	C(23)-C(52)-C(51)	120.001	C(60)-C(30)-C(37)	107.992	C(40)-C(58)-C(41)-	-142.613	C(46)-C(34)-C(33)-	-142.639
C(50)-C(25)	1.453	C(23)-C(52)-C(53)	120.007	C(12)-C(29)-C(11)	108.014	C(40)-C(58)-C(41)-	-0.018	C(44)-C(33)-C(32)-	-138.245
C(49)-C(36)	1.396	C(51)-C(52)-C(53)	108.014	C(12)-C(29)-C(58)	120.007	C(29)-C(58)-C(41)-	0.001	C(44)-C(33)-C(32)-	-0.015
C(49)-C(27)	1.453	C(50)-C(51)-C(48)	120.001	C(11)-C(29)-C(58)	120.001	C(29)-C(58)-C(41)-	142.596	C(34)-C(33)-C(32)-	-0.005
C(48)-C(47)	1.453	C(50)-C(51)-C(52)	119.995	C(27)-C(28)-C(38)	120.010	C(41)-C(58)-C(40)-	-0.015	C(34)-C(33)-C(32)-	138.226
C(48)-C(35)	1.395	C(48)-C(51)-C(52)	107.986	C(27)-C(28)-C(14)	120.013	C(41)-C(58)-C(40)-	142.630	C(41)-C(32)-C(31)-	-0.053
C(47)-C(46)	1.396	C(25)-C(50)-C(49)	108.007	C(38)-C(28)-C(14)	107.999	C(29)-C(58)-C(40)-	-142.633	C(41)-C(32)-C(31)-	-142.620
C(46)-C(45)	1.453	C(25)-C(50)-C(51)	120.006	C(26)-C(27)-C(28)	119.996	C(29)-C(58)-C(40)-	0.012	C(33)-C(32)-C(31)-	142.602
C(46)-C(34)	1.453	C(49)-C(50)-C(51)	120.002	C(26)-C(27)-C(49)	108.002	C(41)-C(58)-C(29)-	0.006	C(33)-C(32)-C(31)-	0.034
C(45)-C(44)	1.453	C(36)-C(49)-C(50)	119.994	C(28)-C(27)-C(49)	119.985	C(41)-C(58)-C(29)-	-138.222	C(32)-C(31)-C(30)-	138.159
C(44)-C(33)	1.453	C(36)-C(49)-C(27)	120.003	C(16)-C(26)-C(27)	119.990	C(40)-C(58)-C(29)-	138.190	C(32)-C(31)-C(30)-	-0.046
C(44)-C(43)	1.396	C(50)-C(49)-C(27)	108.000	C(16)-C(26)-C(25)	119.994	C(40)-C(58)-C(29)-	-0.038	C(40)-C(31)-C(30)-	0.030
C(43)-C(42)	1.453	C(35)-C(48)-C(51)	119.999	C(27)-C(26)-C(25)	107.996	C(10)-C(57)-C(43)-	-0.012	C(40)-C(31)-C(30)-	-138.175
C(42)-C(41)	1.395	C(35)-C(48)-C(47)	120.007	C(24)-C(25)-C(50)	119.995	C(10)-C(57)-C(43)-	-142.605	C(58)-C(29)-C(11)-	-142.615
C(41)-C(32)	1.453	C(51)-C(48)-C(47)	108.017	C(24)-C(25)-C(26)	120.015	C(56)-C(57)-C(43)-	142.582	C(58)-C(29)-C(11)-	-0.016
C(40)-C(31)	1.453	C(46)-C(47)-C(53)	120.020	C(50)-C(25)-C(26)	107.995	C(56)-C(57)-C(43)-	-0.011	C(12)-C(29)-C(11)-	0.040
C(40)-C(39)	1.395	C(46)-C(47)-C(48)	119.986	C(18)-C(24)-C(23)	107.993	C(10)-C(57)-C(56)-	138.177	C(12)-C(29)-C(11)-	142.639
C(39)-C(13)	1.453	C(53)-C(47)-C(48)	107.993	C(18)-C(24)-C(25)	119.988	C(10)-C(57)-C(56)-	-0.045	C(58)-C(29)-C(12)-	0.055
C(39)-C(38)	1.453	C(34)-C(46)-C(45)	107.992	C(23)-C(24)-C(25)	120.001	C(43)-C(57)-C(56)-	0.012	C(58)-C(29)-C(12)-	142.618
C(38)-C(37)	1.395	C(34)-C(46)-C(47)	120.006	C(24)-C(23)-C(52)	120.002	C(43)-C(57)-C(56)-	-138.210	C(11)-C(29)-C(12)-	-142.597
C(38)-C(28)	1.453	C(45)-C(46)-C(47)	119.995	C(24)-C(23)-C(22)	108.003	C(43)-C(57)-C(10)-	0.010	C(11)-C(29)-C(12)-	-0.034
C(37)-C(30)	1.453	C(46)-C(45)-C(55)	119.988	C(52)-C(23)-C(22)	119.991	C(43)-C(57)-C(10)-	142.625	C(38)-C(28)-C(14)-	0.010
C(37)-C(36)	1.453	C(46)-C(45)-C(44)	108.013	C(19)-C(22)-C(21)	120.005	C(56)-C(57)-C(10)-	-142.589	C(38)-C(28)-C(14)-	-142.650
C(36)-C(35)	1.453	C(55)-C(45)-C(44)	120.001	C(19)-C(22)-C(23)	107.998	C(56)-C(57)-C(10)-	0.026	C(27)-C(28)-C(14)-	142.665
C(34)-C(33)	1.453	C(43)-C(44)-C(33)	119.988	C(21)-C(22)-C(23)	120.013	C(57)-C(56)-C(55)-	-142.665	C(27)-C(28)-C(14)-	0.005
C(33)-C(32)	1.395	C(43)-C(44)-C(45)	120.007	C(22)-C(21)-C(54)	119.988	C(57)-C(56)-C(55)-	-0.005	C(14)-C(28)-C(27)-	-138.177
C(32)-C(31)	1.453	C(33)-C(44)-C(45)	107.983	C(22)-C(21)-C(20)	120.001	C(20)-C(56)-C(55)-	-0.010	C(14)-C(28)-C(27)-	-0.012
C(31)-C(30)	1.396	C(44)-C(43)-C(57)	119.990	C(54)-C(21)-C(20)	108.000	C(20)-C(56)-C(55)-	142.650	C(38)-C(28)-C(27)-	0.045
C(29)-C(11)	1.453	C(44)-C(43)-C(42)	119.993	C(8)-C(20)-C(56)	120.006	C(57)-C(56)-C(20)-	142.663	C(38)-C(28)-C(27)-	138.210
C(29)-C(12)	1.453	C(57)-C(43)-C(42)	107.996	C(8)-C(20)-C(21)	119.995	C(57)-C(56)-C(20)-	0.044	C(49)-C(27)-C(26)-	0.012
C(28)-C(14)	1.453	C(41)-C(42)-C(59)	119.995	C(56)-C(20)-C(21)	107.998	C(55)-C(56)-C(20)-	0.007	C(49)-C(27)-C(26)-	142.605
C(28)-C(27)	1.396	C(41)-C(42)-C(43)	120.015	C(7)-C(19)-C(22)	119.988	C(55)-C(56)-C(20)-	-142.612	C(28)-C(27)-C(26)-	-142.582
C(27)-C(26)	1.453	C(59)-C(42)-C(43)	107.995	C(7)-C(19)-C(18)	119.979	C(54)-C(55)-C(45)-	138.223	C(28)-C(27)-C(26)-	0.011
C(26)-C(16)	1.396	C(32)-C(41)-C(42)	119.988	C(22)-C(19)-C(18)	107.994	C(54)-C(55)-C(45)-	0.025	C(25)-C(26)-C(16)-	138.155
C(26)-C(25)	1.453	C(32)-C(41)-C(58)	107.993	C(17)-C(18)-C(24)	119.999	C(56)-C(55)-C(45)-	-0.004	C(25)-C(26)-C(16)-	0.006
C(25)-C(24)	1.395	C(42)-C(41)-C(58)	120.001	C(17)-C(18)-C(19)	120.014	C(56)-C(55)-C(45)-	-138.202	C(27)-C(26)-C(16)-	-0.002
C(24)-C(23)	1.453	C(39)-C(40)-C(31)	120.005	C(24)-C(18)-C(19)	108.011	C(56)-C(55)-C(54)-	142.636	C(27)-C(26)-C(16)-	-138.151
C(24)-C(18)	1.453	C(39)-C(40)-C(58)	120.013	C(6)-C(17)-C(16)	108.011	C(56)-C(55)-C(54)-	0.010	C(27)-C(26)-C(25)-	-0.010
C(23)-C(22)	1.453	C(31)-C(40)-C(58)	107.998	C(6)-C(17)-C(18)	120.004	C(45)-C(55)-C(54)-	-0.013	C(27)-C(26)-C(25)-	142.617
C(22)-C(21)	1.395	C(38)-C(39)-C(13)	108.000	C(16)-C(17)-C(18)	120.016	C(45)-C(55)-C(54)-	-142.639	C(16)-C(26)-C(25)-	-142.602
C(22)-C(19)	1.453	C(38)-C(39)-C(40)	120.001	C(17)-C(16)-C(26)	119.988	C(55)-C(54)-C(53)-	-0.014	C(16)-C(26)-C(25)-	0.025
C(21)-C(20)	1.453	C(13)-C(39)-C(40)	119.988	C(17)-C(16)-C(15)	107.983	C(55)-C(54)-C(53)-	-138.143	C(26)-C(25)-C(24)-	-138.198
C(20)-C(8)	1.395	C(28)-C(38)-C(37)	120.006	C(26)-C(16)-C(15)	120.007	C(21)-C(54)-C(53)-	138.173	C(26)-C(25)-C(24)-	-0.036
C(19)-C(7)	1.396	C(28)-C(38)-C(39)	107.998	C(5)-C(15)-C(14)	119.988	C(21)-C(54)-C(53)-	0.045	C(50)-C(25)-C(24)-	-0.002
C(19)-C(18)	1.453	C(37)-C(38)-C(39)	119.995	C(5)-C(15)-C(16)	108.013	C(55)-C(54)-C(21)-	-0.005	C(50)-C(25)-C(24)-	138.159
C(18)-C(17)	1.395	C(36)-C(37)-C(38)	119.989	C(14)-C(15)-C(16)	120.001	C(55)-C(54)-C(21)-	142.603	C(25)-C(24)-C(23)-	142.613
C(17)-C(16)	1.453	C(36)-C(37)-C(30)	108.015	C(15)-C(14)-C(28)	119.993	C(53)-C(54)-C(21)-	-142.627	C(25)-C(24)-C(23)-	-0.001
C(17)-C(6)	1.453	C(38)-C(37)-C(30)	120.001	C(15)-C(14)-C(13)	120.019	C(53)-C(54)-C(21)-	-0.019	C(18)-C(24)-C(23)-	0.018
C(16)-C(15)	1.453	C(37)-C(36)-C(49)	120.007	C(28)-C(14)-C(13)	108.010	C(54)-C(53)-C(47)-	-142.584	C(18)-C(24)-C(23)-	-142.596
C(15)-C(14)	1.395	C(37)-C(36)-C(35)	107.987	C(12)-C(13)-C(39)	120.009	C(54)-C(53)-C(47)-	0.029	C(25)-C(24)-C(18)-	-142.644
C(15)-C(5)	1.453	C(49)-C(36)-C(35)	119.999	C(12)-C(13)-C(14)	119.998	C(52)-C(53)-C(47)-	-0.015	C(25)-C(24)-C(18)-	0.017
C(14)-C(13)	1.453	C(48)-C(35)-C(60)	120.008	C(39)-C(13)-C(14)	107.993	C(52)-C(53)-C(47)-	142.598	C(23)-C(24)-C(18)-	-0.044
C(13)-C(12)	1.396	C(48)-C(35)-C(36)	120.006	C(4)-C(12)-C(13)	119.979	C(54)-C(53)-C(52)-	142.597	C(23)-C(24)-C(18)-	142.617
C(12)-C(4)	1.453	C(60)-C(35)-C(36)	108.010	C(4)-C(12)-C(29)	107.991	C(54)-C(53)-C(52)-	-0.055	C(52)-C(23)-C(22)-	-0.012
C(11)-C(3)	1.453	C(6)-C(5)-C(4)-C(3)	0.010	C(52)-C(23)-C(22)-	142.633	C(49)-C(50)-C(25)-	-142.632	C(7)-C(19)-C(18)-	142.620
C(10)-C(9)	1.396	C(6)-C(5)-C(4)-C(12)	138.194	C(24)-C(23)-C(22)-	-142.630	C(27)-C(49)-C(36)-	138.180	C(7)-C(19)-C(18)-	-0.034
C(9)-C(8)	1.453	C(15)-C(5)-C(4)-C(3)	-138.167	C(24)-C(23)-C(22)-	0.015	C(27)-C(49)-C(36)-	0.006	C(19)-C(18)-C(17)-	138.245
C(9)-C(2)	1.453	C(15)-C(5)-C(4)-C(12)	0.017	C(23)-C(22)-C(21)-	138.174	C(50)-C(49)-C(36)-	-0.005	C(19)-C(18)-C(17)-	0.005
C(8)-C(7)	1.453	C(12)-C(4)-C(3)-C(11)	0.009	C(23)-C(22)-C(21)-	0.002	C(50)-C(49)-C(36)-	-138.179	C(24)-C(18)-C(17)-	0.015
C(7)-C(1)	1.453	C(12)-C(4)-C(3)-C(2)	-142.644	C(19)-C(22)-C(21)-	-0.039	C(50)-C(49)-C(27)-	142.589	C(24)-C(18)-C(17)-	-138.226

C(6)-C(1)	1.395	C(5)-C(4)-C(3)-C(11)	142.638	C(19)-C(22)-C(21)-	-138.211	C(50)-C(49)-C(27)-	-0.010	C(18)-C(17)-C(16)-	-142.621
C(6)-C(5)	1.453	C(5)-C(4)-C(3)-C(2)	-0.015	C(23)-C(22)-C(19)-	-0.042	C(36)-C(49)-C(27)-	-0.026	C(18)-C(17)-C(16)-	-0.026
C(5)-C(4)	1.396	C(4)-C(3)-C(2)-C(1)	-0.001	C(23)-C(22)-C(19)-	-142.605	C(36)-C(49)-C(27)-	-142.625	C(6)-C(17)-C(16)-	0.044
C(4)-C(3)	1.453	C(4)-C(3)-C(2)-C(9)	138.228	C(21)-C(22)-C(19)-	142.607	C(51)-C(48)-C(47)-	-0.009	C(6)-C(17)-C(16)-	142.639
C(3)-C(2)	1.395	C(11)-C(3)-C(2)-C(1)	-138.233	C(21)-C(22)-C(19)-	0.044	C(51)-C(48)-C(47)-	-142.638	C(18)-C(17)-C(6)-	142.639
C(2)-C(1)	1.453	C(11)-C(3)-C(2)-C(9)	-0.003	C(54)-C(21)-C(20)-	-0.001	C(35)-C(48)-C(47)-	142.644	C(18)-C(17)-C(6)-	0.013
C(13)-C(12)-C(29)	119.992	C(9)-C(2)-C(1)-C(7)	-0.031	C(54)-C(21)-C(20)-	142.623	C(35)-C(48)-C(47)-	0.015	C(16)-C(17)-C(6)-	-0.031
C(29)-C(11)-C(59)	119.995	C(9)-C(2)-C(1)-C(6)	-142.633	C(22)-C(21)-C(20)-	-142.603	C(47)-C(48)-C(35)-	-138.228	C(16)-C(17)-C(6)-	-142.657
C(29)-C(11)-C(3)	107.986	C(3)-C(2)-C(1)-C(7)	142.626	C(22)-C(21)-C(20)-	0.021	C(47)-C(48)-C(35)-	0.001	C(26)-C(16)-C(15)-	-0.005
C(59)-C(11)-C(3)	120.001	C(3)-C(2)-C(1)-C(6)	0.024	C(21)-C(20)-C(8)-	-0.007	C(51)-C(48)-C(35)-	0.003	C(26)-C(16)-C(15)-	-142.627
C(9)-C(10)-C(59)	119.994	C(47)-C(53)-C(52)-C(51)	0.034	C(21)-C(20)-C(8)-	-138.211	C(51)-C(48)-C(35)-	138.232	C(17)-C(16)-C(15)-	142.582
C(9)-C(10)-C(57)	120.003	C(47)-C(53)-C(52)-C(23)	-142.618	C(56)-C(20)-C(8)-	138.181	C(48)-C(47)-C(46)-	138.167	C(17)-C(16)-C(15)-	-0.040
C(59)-C(10)-C(57)	107.999	C(53)-C(52)-C(51)-C(48)	-0.040	C(56)-C(20)-C(8)-	-0.023	C(48)-C(47)-C(46)-	-0.010	C(16)-C(15)-C(14)-	-138.223
C(2)-C(9)-C(8)	107.987	C(53)-C(52)-C(51)-C(50)	-142.639	C(18)-C(19)-C(7)-	-138.159	C(53)-C(47)-C(46)-	-0.017	C(16)-C(15)-C(14)-	0.004
C(2)-C(9)-C(10)	119.999	C(23)-C(52)-C(51)-C(48)	142.615	C(18)-C(19)-C(7)-	0.045	C(53)-C(47)-C(46)-	-138.194	C(5)-C(15)-C(14)-	-0.025
C(8)-C(9)-C(10)	120.007	C(23)-C(52)-C(51)-C(50)	0.016	C(22)-C(19)-C(7)-	-0.030	C(47)-C(46)-C(45)-	-142.637	C(5)-C(15)-C(14)-	138.202
C(9)-C(8)-C(20)	119.989	C(53)-C(52)-C(23)-C(22)	0.038	C(22)-C(19)-C(7)-	138.175	C(47)-C(46)-C(45)-	-0.010	C(16)-C(15)-C(5)-	0.020
C(9)-C(8)-C(7)	108.015	C(53)-C(52)-C(23)-C(24)	138.222	C(22)-C(19)-C(18)-	0.053	C(34)-C(46)-C(45)-	-0.020	C(16)-C(15)-C(5)-	142.637
C(20)-C(8)-C(7)	120.001	C(51)-C(52)-C(23)-C(22)	-138.190	C(22)-C(19)-C(18)-	-142.602	C(34)-C(46)-C(45)-	142.607	C(14)-C(15)-C(5)-	-142.607
C(1)-C(7)-C(19)	120.011	C(51)-C(52)-C(23)-C(24)	-0.006	C(10)-C(9)-C(2)-	142.644	C(47)-C(46)-C(34)-	-0.012	C(14)-C(15)-C(5)-	0.010
C(1)-C(7)-C(8)	107.992	C(52)-C(51)-C(48)-C(47)	0.030	C(10)-C(9)-C(2)-	-0.014	C(47)-C(46)-C(34)-	142.605	C(28)-C(14)-C(13)-	-0.010
C(19)-C(7)-C(8)	120.010	C(52)-C(51)-C(48)-C(35)	-142.627	C(8)-C(9)-C(2)-	0.028	C(45)-C(46)-C(34)-	-142.624	C(28)-C(14)-C(13)-	-142.636
C(1)-C(6)-C(17)	119.989	C(50)-C(51)-C(48)-C(47)	142.627	C(8)-C(9)-C(2)-	-142.629	C(45)-C(46)-C(34)-	-0.007	C(15)-C(14)-C(13)-	142.639
C(1)-C(6)-C(5)	120.009	C(50)-C(51)-C(48)-C(35)	-0.030	C(20)-C(8)-C(7)-	0.012	C(55)-C(45)-C(44)-	-142.581	C(15)-C(14)-C(13)-	0.012
C(17)-C(6)-C(5)	108.001	C(52)-C(51)-C(50)-C(49)	138.197	C(20)-C(8)-C(7)-	-142.630	C(55)-C(45)-C(44)-	0.006	C(14)-C(13)-C(12)-	138.143
C(4)-C(5)-C(15)	119.995	C(52)-C(51)-C(50)-C(25)	-0.019	C(9)-C(8)-C(7)-	142.638	C(46)-C(45)-C(44)-	0.040	C(14)-C(13)-C(12)-	0.015
C(4)-C(5)-C(6)	120.006	C(48)-C(51)-C(50)-C(49)	0.039	C(9)-C(8)-C(7)-	-0.004	C(46)-C(45)-C(44)-	142.627	C(39)-C(13)-C(12)-	-0.045
C(15)-C(5)-C(6)	107.992	C(48)-C(51)-C(50)-C(25)	-138.176	C(8)-C(7)-C(1)-	0.021	C(45)-C(44)-C(33)-	-0.044	C(39)-C(13)-C(12)-	-138.173
C(5)-C(4)-C(12)	120.020	C(51)-C(50)-C(49)-C(27)	-142.641	C(8)-C(7)-C(1)-	142.614	C(45)-C(44)-C(33)-	142.621	C(29)-C(12)-C(4)-	0.015
C(5)-C(4)-C(3)	119.986	C(51)-C(50)-C(49)-C(36)	-0.022	C(19)-C(7)-C(1)-	-142.621	C(43)-C(44)-C(33)-	-142.639	C(29)-C(12)-C(4)-	-142.598
		C(25)-C(50)-C(49)-C(27)	0.004	C(19)-C(7)-C(1)-	-0.028	C(43)-C(44)-C(33)-	0.026	C(13)-C(12)-C(4)-	142.584
		C(25)-C(50)-C(49)-C(36)	142.623	C(5)-C(6)-C(1)-	-0.029	C(45)-C(44)-C(43)-	-138.155	C(13)-C(12)-C(4)-	-0.029
		C(51)-C(50)-C(25)-C(26)	142.647	C(5)-C(6)-C(1)-	-138.192	C(45)-C(44)-C(43)-	0.002	C(59)-C(11)-C(3)-	-142.627
		C(51)-C(50)-C(25)-C(24)	0.012	C(17)-C(6)-C(1)-	138.160	C(33)-C(44)-C(43)-	-0.006	C(59)-C(11)-C(3)-	0.030
		C(49)-C(50)-C(25)-C(26)	0.004	C(17)-C(6)-C(1)-	-0.002	C(33)-C(44)-C(43)-	138.151	C(29)-C(11)-C(3)-	-0.030
		C(58)-C(41)-C(32)-C(33)	-142.617	C(17)-C(6)-C(5)-	0.007	C(57)-C(43)-C(42)-	0.010	C(29)-C(11)-C(3)-	142.627
		C(42)-C(41)-C(32)-C(31)	142.644	C(17)-C(6)-C(5)-	-142.605	C(57)-C(43)-C(42)-	-142.617	C(57)-C(10)-C(9)-	-0.006
		C(42)-C(41)-C(32)-C(33)	-0.017	C(31)-C(40)-C(39)-	138.211	C(44)-C(43)-C(42)-	142.602	C(57)-C(10)-C(9)-	-138.180
		C(58)-C(40)-C(31)-C(32)	0.042	C(31)-C(40)-C(39)-	0.039	C(44)-C(43)-C(42)-	-0.025	C(59)-C(10)-C(9)-	138.179
		C(58)-C(40)-C(31)-C(30)	142.605	C(40)-C(39)-C(13)-	-142.603	C(43)-C(42)-C(41)-	138.198	C(59)-C(10)-C(9)-	0.005
		C(39)-C(40)-C(31)-C(32)	-142.607	C(40)-C(39)-C(13)-	0.019	C(43)-C(42)-C(41)-	0.037	C(10)-C(9)-C(8)-	-142.627
		C(39)-C(40)-C(31)-C(30)	-0.044	C(38)-C(39)-C(13)-	0.005	C(59)-C(42)-C(41)-	0.002	C(10)-C(9)-C(8)-	0.005
		C(58)-C(40)-C(39)-C(13)	-0.002	C(38)-C(39)-C(13)-	142.627	C(59)-C(42)-C(41)-	-138.159	C(2)-C(9)-C(8)-C(7)	-0.015
		C(58)-C(40)-C(39)-C(38)	-138.174	C(40)-C(39)-C(38)-	-0.021	C(58)-C(41)-C(32)-	0.044	C(2)-C(9)-C(8)-	142.617
		C(1)-C(6)-C(5)-C(4)	0.012	C(40)-C(39)-C(38)-	142.603	C(13)-C(39)-C(38)-	-142.623	C(1)-C(6)-C(5)-	142.624

Table S2. The calculated geometric parameters at the four different levels of the $C_{60}Cl_6$ molecule. Bond lengths in Angstrom (Å) and angles in Degrees (º).

	Method/Basis set					Method/Basis set					Method/Basis set			
Bond Lenght	**B3LYP/6-31G(d,p)**	**RM062X/6-31G(d,p)**	**HSEH1PBE/6-31G(d,p)**	**B3LYP/6-311++G(d,p)**	***Bond Angles***	**B3LYP/6-31G(d,p)**	**RM062X/6-31G(d,p)**	**HSEH1PBE/6-31G(d,p)**	**B3LYP/6-311++G(d,p)**	***Dihedral Angles***	**B3LYP/6-31G(d,p)**	**RM062X/6-31G(d,p)**	**HSEH1PBE/6-31G(d,p)**	**B3LYP/6-311++G(d,p)**
(C1,C2)	1.54	1.54	1.53	1.54	(C2,C1,C6)	114.5	114.4	114.4	114.5	(C6,C1,C2,C3)	25.2	26.3	25.8	24.9
(C1,C6)	1.58	1.57	1.57	1.58	(C2,C1,C7)	100.9	100.6	100.9	100.9	(C6,C1,C2,C9)	-137.5	-137.9	-137.8	-137.5
(C1,C7)	1.54	1.54	1.53	1.54	(C2,C1,Cl62)	106.4	106.7	106.5	106.3	(C7,C1,C2,C3)	148.6	149.4	149.2	148.4
(C1,Cl62)	1.84	1.81	1.81	1.84	(C6,C1,C7)	114.5	114.4	114.4	114.5	(C7,C1,C2,C9)	-14.1	-14.8	-14.4	-13.9
(C2,C3)	1.49	1.49	1.49	1.49	(C6,C1,Cl62)	113.1	113.0	113.0	113.1	(Cl62,C1,C2,C3)	-100.5	-99.4	-99.8	-100.8
(C2,C9)	1.35	1.34	1.34	1.34	(C7,C1,Cl62)	106.4	106.7	106.5	106.3	(Cl62,C1,C2,C9)	96.8	96.4	96.7	96.8
(C3,C4)	1.53	1.52	1.52	1.52	(C1,C2,C3)	125.5	125.6	125.7	125.4	(C2,C1,C6,C5)	1.1	1.2	1.3	1.1
(C3,C11)	1.54	1.54	1.53	1.54	(C1,C2,C9)	108.9	109.1	108.9	108.9	(C2,C1,C6,C17)	114.7	114.2	114.5	114.8
(C3,Cl61)	1.85	1.81	1.82	1.85	(C3,C2,C9)	123.2	123.4	123.2	123.2	(C2,C1,C6,Cl63)	-122.1	-122.3	-122.1	-122.0
(C4,C5)	1.37	1.37	1.37	1.37	(C2,C3,C4)	108.5	107.7	107.9	108.6	(C7,C1,C6,C5)	-114.7	-114.2	-114.5	-114.8
(C4,C12)	1.44	1.44	1.44	1.44	(C2,C3,C11)	109.8	109.2	109.4	109.9	(C7,C1,C6,C17)	-1.1	-1.2	-1.3	-1.1
(C5,C6)	1.53	1.53	1.52	1.53	(C2,C3,Cl61)	113.3	113.1	113.6	113.2	(C7,C1,C6,Cl63)	122.1	122.3	122.1	122.0
(C5,C15)	1.44	1.44	1.43	1.44	(C4,C3,C11)	101.2	100.9	101.0	101.3	(Cl62,C1,C6,C5)	123.2	123.5	123.4	123.1
(C6,C17)	1.53	1.53	1.52	1.53	(C4,C3,Cl61)	111.7	112.3	112.0	111.5	(Cl62,C1,C6,C17)	-123.2	-123.5	-123.4	-123.1
(C6,Cl63)	1.84	1.81	1.82	1.84	(C11,C3,Cl61)	111.7	112.8	112.1	111.6	(Cl62,C1,C6,Cl63)	0.0	0.0	0.0	0.0
(C7,C8)	1.35	1.34	1.34	1.34	(C3,C4,C5)	123.8	123.8	123.8	123.8	(C2,C1,C7,C8)	14.1	14.8	14.4	13.9
(C7,C19)	1.49	1.49	1.49	1.49	(C3,C4,C12)	109.8	109.9	109.9	109.7	(C2,C1,C7,C19)	-148.6	-149.4	-149.2	-148.4
(C8,C9)	1.47	1.47	1.46	1.47	(C5,C4,C12)	119.5	119.6	119.5	119.6	(C6,C1,C7,C8)	137.5	137.9	137.8	137.5
(C8,C20)	1.50	1.50	1.49	1.49	(C4,C5,C6)	126.2	126.4	126.3	126.2	(C6,C1,C7,C19)	-25.2	-26.3	-25.8	-24.9
(C9,C10)	1.50	1.50	1.49	1.49	(C4,C5,C15)	119.7	119.7	119.7	119.7	(Cl62,C1,C7,C8)	-96.8	-96.4	-96.7	-96.8
(C10,C57)	1.52	1.52	1.52	1.52	(C6,C5,C15)	109.0	109.1	109.1	109.0	(Cl62,C1,C7,C19)	100.5	99.4	99.8	100.8
(C10,C59)	1.53	1.52	1.52	1.52	(C1,C6,C5)	112.8	112.6	112.7	112.9	(C2,C1,Cl62,Cl63)	126.5	126.6	126.4	126.5
(C10,Cl66)	1.85	1.81	1.82	1.85	(C1,C6,C17)	112.8	112.6	112.7	112.9	(C6,C1,Cl62,Cl63)	0.0	0.0	0.0	0.0
(C11,C29)	1.44	1.44	1.43	1.44	(C1,C6,Cl63)	114.4	114.4	114.4	114.4	(C7,C1,Cl62,Cl63)	-126.5	-126.6	-126.4	-126.5
(C11,C59)	1.37	1.37	1.37	1.37	(C5,C6,C17)	100.9	100.7	100.8	101.0	(C1,C2,C3,C4)	-35.1	-36.5	-36.0	-34.7
(C12,C13)	1.40	1.39	1.39	1.39	(C5,C6,Cl63)	107.4	107.8	107.7	107.3	(C1,C2,C3,C11)	-144.8	-145.3	-145.0	-144.6
(C12,C29)	1.45	1.45	1.44	1.45	(C17,C6,Cl63)	107.4	107.8	107.7	107.3	(C1,C2,C3,Cl61)	89.5	88.2	88.8	89.8
(C13,C14)	1.44	1.44	1.44	1.44	(C1,C7,C8)	108.9	109.1	108.9	108.9	(C9,C2,C3,C4)	125.3	125.5	125.3	125.3
(C13,C39)	1.45	1.45	1.45	1.45	(C1,C7,C19)	125.5	125.6	125.7	125.4	(C9,C2,C3,C11)	15.6	16.7	16.3	15.3
(C14,C15)	1.39	1.39	1.39	1.39	(C8,C7,C19)	123.2	123.4	123.2	123.2	(C9,C2,C3,Cl61)	-110.1	-109.7	-109.8	-110.2
(C14,C28)	1.45	1.45	1.44	1.45	(C7,C8,C9)	109.6	109.4	109.5	109.6	(C1,C2,C9,C8)	9.5	9.9	9.7	9.4
(C15,C16)	1.45	1.45	1.44	1.44	(C7,C8,C20)	125.3	125.5	125.4	125.3	(C1,C2,C9,C10)	170.9	171.8	171.7	170.5
(C16,C17)	1.44	1.44	1.43	1.44	(C9,C8,C20)	122.4	122.4	122.5	122.3	(C3,C2,C9,C8)	-153.7	-154.7	-154.4	-153.5
(C16,C26)	1.39	1.39	1.39	1.39	(C2,C9,C8)	109.6	109.4	109.5	109.6	(C3,C2,C9,C10)	7.7	7.2	7.6	7.6
(C17,C18)	1.37	1.37	1.37	1.37	(C2,C9,C10)	125.3	125.5	125.4	125.3	(C2,C3,C4,C5)	20.5	21.3	21.1	20.3
(C18,C19)	1.53	1.52	1.52	1.52	(C8,C9,C10)	122.4	122.4	122.5	122.3	(C2,C3,C4,C12)	-130.1	-129.6	-129.8	-130.3
(C18,C24)	1.44	1.44	1.44	1.44	(C9,C10,C57)	109.5	109.0	109.1	109.7	(C11,C3,C4,C5)	136.0	135.7	135.8	136.0
(C19,C22)	1.54	1.54	1.53	1.54	(C9,C10,C59)	108.9	108.3	108.5	109.1	(C11,C3,C4,C12)	-14.7	-15.2	-15.1	-14.6
(C19,Cl64)	1.85	1.81	1.82	1.85	(C9,C10,Cl66)	111.0	111.2	111.3	110.9	(Cl61,C3,C4,C5)	-105.1	-103.9	-104.7	-105.2
(C20,C21)	1.53	1.52	1.52	1.52	(C57,C10,C59)	102.3	102.1	102.2	102.4	(Cl61,C3,C4,C12)	104.3	105.1	104.4	104.3
(C20,C56)	1.52	1.52	1.52	1.52	(C57,C10,Cl66	111.9	112.3	112.2	111.7	(C2,C3,C11,C29)	128.8	128.2	128.4	129.0
(C20,Cl65)	1.85	1.81	1.82	1.85	(C59,C10,Cl66	112.8	113.4	113.2	112.7	(C2,C3,C11,C59)	-20.0	-20.8	-20.7	-19.7
(C21,C22)	1.37	1.37	1.37	1.37	(C3,C11,C29)	109.6	109.6	109.7	109.5	(C4,C3,C11,C29)	14.4	14.9	14.7	14.3
(C21,C54)	1.44	1.44	1.43	1.44	(C3,C11,C59)	123.4	123.5	123.5	123.4	(C4,C3,C11,C59)	-134.4	-134.1	-134.3	-134.5
(C22,C23)	1.44	1.44	1.43	1.44	(C29,C11,C59)	119.3	119.2	119.2	119.3	(Cl61,C3,C11,C29)	-104.6	-105.1	-104.6	-104.5
(C23,C24)	1.45	1.45	1.44	1.45	(C4,C12,C13)	121.2	121.2	121.3	121.2	(Cl61,C3,C11,C59)	106.6	105.9	106.3	106.8
(C23,C52)	1.40	1.39	1.40	1.40	(C4,C12,C29)	108.5	108.4	108.4	108.5	(C3,C4,C5,C6)	2.9	2.9	2.8	2.9
(C24,C25)	1.40	1.39	1.39	1.39	(C13,C12,C29)	120.1	120.1	120.2	120.2	(C3,C4,C5,C15)	-149.0	-149.7	-149.4	-149.0
(C25,C26)	1.44	1.44	1.44	1.44	(C12,C13,C14)	119.1	119.1	119.0	119.1	(C12,C4,C5,C6)	150.9	151.3	151.1	150.8
(C25,C50)	1.45	1.45	1.45	1.45	(C12,C13,C39)	120.3	120.3	120.3	120.3	(C12,C4,C5,C15)	-1.1	-1.3	-1.2	-1.1
(C26,C27)	1.45	1.45	1.44	1.45	(C14,C13,C39)	108.0	108.0	108.0	108.0	(C3,C4,C12,C13)	155.4	155.6	155.6	155.3

(C27,C28)	1.40	1.39	1.39	1.39
(C27,C49)	1.45	1.45	1.44	1.45
(C28,C38)	1.45	1.45	1.44	1.45
(C29,C58)	1.40	1.39	1.40	1.40
(C30,C31)	1.40	1.39	1.40	1.40
(C30,C37)	1.45	1.45	1.45	1.45
(C30,C60)	1.45	1.45	1.45	1.45
(C31,C32)	1.45	1.45	1.44	1.45
(C31,C40)	1.45	1.45	1.45	1.45
(C32,C33)	1.40	1.39	1.39	1.39
(C32,C41)	1.45	1.45	1.45	1.45
(C33,C34)	1.45	1.45	1.45	1.45
(C33,C44)	1.45	1.45	1.45	1.45
(C34,C46)	1.45	1.45	1.45	1.45
(C34,C60)	1.40	1.39	1.39	1.40
(C35,C36)	1.45	1.45	1.45	1.45
(C35,C48)	1.40	1.39	1.40	1.40
(C35,C60)	1.45	1.45	1.45	1.45
(C36,C37)	1.45	1.45	1.45	1.45
(C36,C49)	1.40	1.39	1.39	1.40
(C37,C38)	1.40	1.39	1.39	1.40
(C38,C39)	1.45	1.45	1.45	1.45
(C39,C40)	1.39	1.39	1.39	1.39
(C40,C58)	1.45	1.45	1.45	1.45
(C41,C42)	1.40	1.39	1.39	1.39
(C41,C58)	1.44	1.44	1.43	1.44
(C42,C43)	1.45	1.45	1.45	1.45
(C42,C59)	1.44	1.44	1.43	1.44
(C43,C44)	1.40	1.39	1.39	1.39
(C43,C57)	1.43	1.43	1.43	1.43
(C44,C45)	1.44	1.44	1.43	1.44
(C45,C46)	1.45	1.45	1.45	1.45
(C45,C55)	1.40	1.39	1.39	1.39
(C46,C47)	1.40	1.39	1.39	1.39
(C47,C48)	1.45	1.45	1.44	1.45
(C47,C53)	1.45	1.45	1.45	1.45
(C48,C51)	1.45	1.45	1.45	1.45
(C49,C50)	1.45	1.45	1.45	1.45
(C50,C51)	1.39	1.39	1.39	1.39
(C51,C52)	1.45	1.45	1.45	1.45
(C52,C53)	1.44	1.44	1.43	1.44
(C53,C54)	1.40	1.39	1.39	1.39
(C54,C55)	1.45	1.45	1.45	1.45
(C55,C56)	1.43	1.43	1.43	1.43
(C56,C57)	1.38	1.37	1.37	1.37
(Cl62,Cl63	3.06	3.03	3.03	3.06

(C13,C14,C15)	119.0	119.0	119.0	119.0
(C13,C14,C28)	108.4	108.4	108.4	108.4
(C15,C14,C28)	120.0	119.9	119.9	119.9
(C5,C15,C14)	121.4	121.3	121.4	121.3
(C5,C15,C16)	108.5	108.4	108.4	108.5
(C14,C15,C16)	120.1	120.1	120.1	120.1
(C15,C16,C17)	108.5	108.4	108.4	108.5
(C15,C16,C26)	120.1	120.1	120.1	120.1
(C17,C16,C26)	121.4	121.3	121.4	121.3
(C6,C17,C16)	109.0	109.1	109.1	109.0
(C6,C17,C18)	126.2	126.4	126.3	126.2
(C16,C17,C18)	119.7	119.7	119.7	119.7
(C17,C18,C19)	123.8	123.8	123.8	123.8
(C17,C18,C24)	119.5	119.6	119.5	119.6
(C19,C18,C24)	109.8	109.9	109.9	109.7
(C7,C19,C18)	108.5	107.7	107.9	108.6
(C7,C19,C22)	109.8	109.2	109.4	109.9
(C7,C19,Cl64)	113.3	113.1	113.6	113.2
(C18,C19,C22)	101.2	100.9	101.0	101.3
(C18,C19,Cl64	111.7	112.3	112.0	111.5
(C22,C19,Cl64	111.7	112.8	112.1	111.6
(C8,C20,C21)	108.9	108.3	108.5	109.1
(C8,C20,C56)	109.5	109.0	109.1	109.7
(C8,C20,Cl65)	111.0	111.2	111.3	110.9
(C21,C20,C56)	102.3	102.1	102.2	102.4
(C21,C20,Cl65	112.8	113.4	113.2	112.7
(C56,C20,Cl65	111.9	112.3	112.2	111.7
(C20,C21,C22)	122.2	122.4	122.3	122.2
(C20,C21,C54)	109.2	109.3	109.3	109.2
(C22,C21,C54)	120.2	120.2	120.2	120.2
(C19,C22,C21)	123.4	123.5	123.5	123.4
(C19,C22,C23)	109.6	109.6	109.7	109.5
(C21,C22,C23)	119.3	119.2	119.2	119.3
(C22,C23,C24)	108.6	108.6	108.6	108.7
(C22,C23,C52)	121.2	121.2	121.3	121.2
(C24,C23,C52)	119.6	119.5	119.5	119.6
(C18,C24,C23)	108.5	108.4	108.4	108.5
(C18,C24,C25)	121.2	121.2	121.3	121.2
(C23,C24,C25)	120.1	120.1	120.2	120.2
(C24,C25,C26)	119.1	119.1	119.0	119.1
(C24,C25,C50)	120.3	120.3	120.3	120.3
(C26,C25,C50)	108.0	108.0	108.0	108.0
(C16,C26,C25)	119.0	119.0	119.0	119.0
(C16,C26,C27)	120.0	119.9	119.9	119.9
(C25,C26,C27)	108.4	108.4	108.4	108.4
(C26,C27,C28)	119.9	120.0	120.0	120.0
(C26,C27,C49)	107.8	107.8	107.8	107.8
(C28,C27,C49)	120.1	120.1	120.1	120.1
(C14,C28,C27)	119.9	120.0	120.0	120.0
(C14,C28,C38)	107.8	107.8	107.8	107.8
(C27,C28,C38)	120.1	120.1	120.1	120.1
(C11,C29,C12)	108.6	108.6	108.6	108.7
(C11,C29,C58)	121.2	121.2	121.3	121.2
(C12,C29,C58)	119.6	119.5	119.5	119.6
(C31,C30,C37)	119.9	119.9	119.9	119.9
(C31,C30,C60)	120.0	120.0	120.0	120.0
(C37,C30,C60)	107.9	108.0	108.0	107.9
(C30,C31,C32)	120.0	120.0	120.0	120.0
(C30,C31,C40)	120.2	120.2	120.2	120.1

(C3,C4,C12,C29)	10.1	10.5	10.4	10.0
(C5,C4,C12,C13)	3.3	3.3	3.3	3.4
(C5,C4,C12,C29)	-142.0	-141.9	-142.0	-142.0
(C4,C5,C6,C1)	-14.4	-15.0	-14.7	-14.3
(C4,C5,C6,C17)	-135.0	-135.1	-135.0	-135.0
(C4,C5,C6,Cl63)	112.6	112.1	112.3	112.7
(C15,C5,C6,C1)	140.0	140.0	139.9	140.1
(C15,C5,C6,C17)	19.4	19.9	19.6	19.3
(C15,C5,C6,Cl63)	-93.0	-92.9	-93.1	-92.9
(C4,C5,C15,C14)	-1.9	-1.5	-1.8	-1.9
(C4,C5,C15,C16)	143.5	143.7	143.5	143.5
(C6,C5,C15,C14)	-158.2	-158.4	-158.3	-158.2
(C6,C5,C15,C16)	-12.9	-13.2	-13.0	-12.8
(C1,C6,C17,C16)	-140.0	-140.0	-139.9	-140.1
(C1,C6,C17,C18)	14.4	15.0	14.7	14.3
(C5,C6,C17,C16)	-19.4	-19.9	-19.6	-19.3
(C5,C6,C17,C18)	135.0	135.1	135.0	135.0
(Cl63,C6,C17,C16)	93.0	92.9	93.1	92.9
(Cl63,C6,C17,C18)	-112.6	-112.1	-112.3	-112.7
(C1,C6,Cl63,Cl62)	0.0	0.0	0.0	0.0
(C5,C6,Cl63,Cl62)	-126.1	-126.0	-126.0	-126.1
(C17,C6,Cl63,Cl62)	126.1	126.0	126.0	126.1
(C1,C7,C8,C9)	-9.5	-9.9	-9.7	-9.4
(C1,C7,C8,C20)	-170.9	-171.8	-171.7	-170.5
(C19,C7,C8,C9)	153.7	154.7	154.4	153.5
(C19,C7,C8,C20)	-7.7	-7.2	-7.6	-7.6
(C1,C7,C19,C18)	35.1	36.5	36.0	34.7
(C1,C7,C19,C22)	144.8	145.3	145.0	144.6
(C1,C7,C19,Cl64)	-89.5	-88.2	-88.8	-89.8
(C8,C7,C19,C18)	-125.3	-125.5	-125.3	-125.3
(C8,C7,C19,C22)	-15.6	-16.7	-16.3	-15.3
(C8,C7,C19,Cl64)	110.1	109.7	109.8	110.2
(C7,C8,C9,C2)	0.0	0.0	0.0	0.0
(C7,C8,C9,C10)	-162.1	-162.5	-162.7	-161.8
(C20,C8,C9,C2)	162.1	162.5	162.7	161.8
(C20,C8,C9,C10)	0.0	0.0	0.0	0.0
(C7,C8,C20,C21)	25.6	26.1	26.3	25.3
(C7,C8,C20,C56)	136.8	136.5	136.8	136.7
(C7,C8,C20,Cl65)	-99.2	-99.2	-98.9	-99.4
(C9,C8,C20,C21)	-133.5	-133.5	-133.6	-133.5
(C9,C8,C20,C56)	-22.4	-23.1	-23.0	-22.1
(C9,C8,C20,Cl65)	101.7	101.2	101.3	101.7
(C2,C9,C10,C57)	-136.8	-136.5	-136.8	-136.7
(C2,C9,C10,C59)	-25.6	-26.1	-26.3	-25.3
(C2,C9,C10,Cl66)	99.2	99.2	98.9	99.4
(C8,C9,C10,C57)	22.4	23.1	23.0	22.1
(C8,C9,C10,C59)	133.5	133.5	133.6	133.5
(C8,C9,C10,Cl66)	-101.7	-101.2	-101.3	-101.7
(C9,C10,C57,C43)	127.9	127.5	127.5	128.1
(C9,C10,C57,C56)	-22.8	-23.6	-23.4	-22.5
(C59,C10,C57,C43)	12.4	13.0	12.7	12.4
(C59,C10,C57,C56)	-138.2	-138.0	-138.1	-138.3
(Cl66,C10,C57,C43	-108.6	-108.8	-108.8	-108.5
(Cl66,C10,C57,C56	100.8	100.1	100.3	100.9
(C9,C10,C59,C11)	20.3	21.1	21.0	20.1
(C9,C10,C59,C42)	-127.7	-127.3	-127.3	-127.9
(C57,C10,C59,C11)	136.2	136.1	136.1	136.2
(C57,C10,C59,C42)	-11.9	-12.4	-12.2	-11.8
(Cl66,C10,C59,C11	-103.4	-102.9	-103.1	-103.6

(C32,C31,C40)	107.8	107.8	107.8	107.8	(Cl66,C10,C59,C42	108.5	108.7	108.7	108.4
(C31,C32,C33)	119.9	119.9	119.9	119.9	(C3,C11,C29,C12)	-9.3	-9.6	-9.5	-9.2
(C31,C32,C41)	107.9	107.9	107.9	107.9	(C3,C11,C29,C58)	-153.6	-153.8	-153.9	-153.6
(C33,C32,C41)	120.1	120.2	120.1	120.1	(C59,C11,C29,C12)	141.0	140.9	141.1	141.0
(C32,C33,C34)	120.2	120.2	120.2	120.2	(C59,C11,C29,C58)	-3.3	-3.3	-3.3	-3.4
(C32,C33,C44)	119.8	119.8	119.8	119.9	(C3,C11,C59,C10)	1.6	1.4	1.6	1.6
(C34,C33,C44)	107.8	107.8	107.8	107.8	(C3,C11,C59,C42)	146.3	146.6	146.5	146.2
(C33,C34,C46)	107.9	108.0	107.9	107.9	(C29,C11,C59,C10)	-144.4	-144.8	-144.7	-144.3
(C33,C34,C60)	119.9	119.9	120.0	119.9	(C29,C11,C59,C42)	0.3	0.4	0.3	0.3
(C46,C34,C60)	119.9	119.9	120.0	119.9	(C4,C12,C13,C14)	-2.6	-2.3	-2.5	-2.6
(C36,C35,C48)	119.9	119.9	119.9	119.9	(C4,C12,C13,C39)	-139.8	-139.6	-139.6	-139.7
(C36,C35,C60)	107.9	108.0	108.0	107.9	(C29,C12,C13,C14)	138.8	138.8	138.8	138.8
(C48,C35,C60)	120.0	120.0	120.0	120.0	(C29,C12,C13,C39)	1.6	1.5	1.7	1.7
(C35,C36,C37)	108.0	108.0	108.0	108.0	(C4,C12,C29,C11)	-0.4	-0.5	-0.5	-0.5
(C35,C36,C49)	119.9	119.8	119.9	119.9	(C4,C12,C29,C58)	144.6	144.4	144.6	144.6
(C37,C36,C49)	120.1	120.0	120.1	120.1	(C13,C12,C29,C11)	-146.2	-146.1	-146.2	-146.2
(C30,C37,C36)	108.0	108.0	108.0	108.0	(C13,C12,C29,C58)	-1.1	-1.1	-1.1	-1.1
(C30,C37,C38)	119.9	119.8	119.9	119.9	(C12,C13,C14,C15)	-0.4	-0.5	-0.4	-0.4
(C36,C37,C38)	120.1	120.0	120.1	120.1	(C12,C13,C14,C28)	-142.2	-142.3	-142.1	-142.1
(C28,C38,C37)	119.8	119.8	119.8	119.8	(C39,C13,C14,C15)	141.5	141.5	141.5	141.5
(C28,C38,C39)	107.9	107.9	107.9	107.9	(C39,C13,C14,C28)	-0.3	-0.3	-0.3	-0.2
(C37,C38,C39)	120.1	120.1	120.1	120.1	(C12,C13,C39,C38)	141.4	141.6	141.4	141.4
(C13,C39,C38)	107.9	107.9	107.9	107.9	(C12,C13,C39,C40)	-0.8	-0.8	-0.9	-0.9
(C13,C39,C40)	119.7	119.7	119.7	119.7	(C14,C13,C39,C38)	0.1	0.1	0.1	0.1
(C38,C39,C40)	120.1	120.1	120.1	120.1	(C14,C13,C39,C40)	-142.2	-142.2	-142.2	-142.2
(C31,C40,C39)	119.9	119.9	119.9	119.9	(C13,C14,C15,C5)	2.6	2.4	2.6	2.6
(C31,C40,C58)	108.1	108.1	108.1	108.1	(C13,C14,C15,C16)	-138.8	-138.8	-138.8	-138.8
(C39,C40,C58)	120.0	120.0	120.0	120.0	(C28,C14,C15,C5)	140.0	139.8	139.8	139.9
(C32,C41,C42)	120.1	120.1	120.1	120.1	(C28,C14,C15,C16)	-1.5	-1.5	-1.6	-1.6
(C32,C41,C58)	108.3	108.3	108.3	108.3	(C13,C14,C28,C27)	142.8	142.8	142.8	142.8
(C42,C41,C58)	119.0	119.0	118.9	119.0	(C13,C14,C28,C38)	0.3	0.3	0.3	0.3
(C41,C42,C43)	119.6	119.6	119.6	119.6	(C15,C14,C28,C27)	1.5	1.5	1.5	1.6
(C41,C42,C59)	121.0	121.0	121.1	121.0	(C15,C14,C28,C38)	-141.0	-141.0	-141.0	-141.0
(C43,C42,C59)	108.8	108.8	108.8	108.8	(C5,C15,C16,C17)	0.0	0.0	0.0	0.0
(C42,C43,C44)	120.3	120.3	120.3	120.3	(C5,C15,C16,C26)	-145.9	-145.7	-145.9	-145.9
(C42,C43,C57)	108.7	108.6	108.6	108.7	(C14,C15,C16,C17)	145.9	145.7	145.9	145.9
(C44,C43,C57)	120.8	120.8	120.9	120.8	(C14,C15,C16,C26)	0.0	0.0	0.0	0.0
(C33,C44,C43)	120.0	120.0	120.0	119.9	(C15,C16,C17,C6)	12.9	13.2	13.0	12.8
(C33,C44,C45)	108.2	108.2	108.2	108.2	(C15,C16,C17,C18)	-143.5	-143.7	-143.5	-143.5
(C43,C44,C45)	119.3	119.3	119.3	119.3	(C26,C16,C17,C6)	158.2	158.4	158.3	158.2
(C44,C45,C46)	108.2	108.2	108.2	108.2	(C26,C16,C17,C18)	1.9	1.5	1.8	1.9
(C44,C45,C55)	119.3	119.3	119.3	119.3	(C15,C16,C26,C25)	138.8	138.8	138.8	138.8
(C46,C45,C55)	120.0	120.0	120.0	119.9	(C15,C16,C26,C27)	1.5	1.5	1.6	1.6
(C34,C46,C45)	107.8	107.8	107.8	107.8	(C17,C16,C26,C25)	-2.6	-2.4	-2.6	-2.6
(C34,C46,C47)	120.2	120.2	120.2	120.2	(C17,C16,C26,C27)	-140.0	-139.8	-139.8	-139.9
(C45,C46,C47)	119.8	119.8	119.8	119.9	(C6,C17,C18,C19)	-2.9	-2.9	-2.8	-2.9
(C46,C47,C48)	119.9	119.9	119.9	119.9	(C6,C17,C18,C24)	-150.9	-151.3	-151.1	-150.8
(C46,C47,C53)	120.1	120.2	120.1	120.1	(C16,C17,C18,C19)	149.0	149.7	149.4	149.0
(C48,C47,C53)	107.9	107.9	107.9	107.9	(C16,C17,C18,C24)	1.1	1.3	1.2	1.1
(C35,C48,C47)	120.0	120.0	120.0	120.0	(C17,C18,C19,C7)	-20.5	-21.3	-21.1	-20.3
(C35,C48,C51)	120.2	120.2	120.2	120.1	(C17,C18,C19,C22)	-136.0	-135.7	-135.8	-136.0
(C47,C48,C51)	107.8	107.8	107.8	107.8	(C17,C18,C19,Cl64	105.1	103.9	104.7	105.2
(C27,C49,C36)	119.8	119.8	119.8	119.8	(C24,C18,C19,C7)	130.1	129.6	129.8	130.3
(C27,C49,C50)	107.9	107.9	107.9	107.9	(C24,C18,C19,C22)	14.7	15.2	15.1	14.6
(C36,C49,C50)	120.1	120.1	120.1	120.1	(C24,C18,C19,Cl64	-104.3	-105.1	-104.4	-104.3
(C25,C50,C49)	107.9	107.9	107.9	107.9	(C17,C18,C24,C23)	142.0	141.9	142.0	142.0
(C25,C50,C51)	119.7	119.7	119.7	119.7	(C17,C18,C24,C25)	-3.3	-3.3	-3.3	-3.4
(C49,C50,C51)	120.1	120.1	120.1	120.1	(C19,C18,C24,C23)	-10.1	-10.5	-10.4	-10.0
(C48,C51,C50)	119.9	119.9	119.9	119.9	(C19,C18,C24,C25)	-155.4	-155.6	-155.6	-155.3

(C48,C51,C52)	108.1	108.1	108.1	108.1
(C50,C51,C52)	120.0	120.0	120.0	120.0
(C23,C52,C51)	120.3	120.3	120.3	120.2
(C23,C52,C53)	119.2	119.2	119.2	119.2
(C51,C52,C53)	108.0	108.0	108.0	108.0
(C47,C53,C52)	108.3	108.3	108.3	108.3
(C47,C53,C54)	120.1	120.1	120.1	120.1
(C52,C53,C54)	119.0	119.0	118.9	119.0
(C21,C54,C53)	121.0	121.0	121.1	121.0
(C21,C54,C55)	108.8	108.8	108.8	108.8
(C53,C54,C55)	119.6	119.6	119.6	119.6
(C45,C55,C54)	120.3	120.3	120.3	120.3
(C45,C55,C56)	120.8	120.8	120.9	120.8
(C54,C55,C56)	108.7	108.6	108.6	108.7
(C20,C56,C55)	109.4	109.4	109.4	109.3
(C20,C56,C57)	123.8	124.0	123.9	123.8
(C55,C56,C57)	119.9	119.9	119.9	119.9
(C10,C57,C43)	109.4	109.4	109.4	109.3
(C10,C57,C56)	123.8	124.0	123.9	123.8
(C43,C57,C56)	119.9	119.9	119.9	119.9
(C29,C58,C40)	120.3	120.3	120.3	120.2
(C29,C58,C41)	119.2	119.2	119.2	119.2
(C40,C58,C41)	108.0	108.0	108.0	108.0
(C10,C59,C11)	122.2	122.4	122.3	122.2
(C10,C59,C42)	109.2	109.3	109.3	109.2
(C11,C59,C42)	120.2	120.2	120.2	120.2
(C30,C60,C34)	119.9	119.9	119.9	119.9
(C30,C60,C35)	108.1	108.1	108.1	108.1
(C34,C60,C35)	119.9	119.9	119.9	119.9
(C1,Cl62,Cl63)	66.7	66.7	66.8	66.7
(C6,Cl63,Cl62)	65.8	65.9	65.9	65.8

(C7,C19,C22,C21)	20.0	20.8	20.7	19.7
(C7,C19,C22,C23)	-128.8	-128.2	-128.4	-129.0
(C18,C19,C22,C21)	134.4	134.1	134.3	134.5
(C18,C19,C22,C23)	-14.4	-14.9	-14.7	-14.3
(Cl64,C19,C22,C21	-106.6	-105.9	-106.3	-106.8
(Cl64,C19,C22,C23	104.6	105.1	104.6	104.5
(C8,C20,C21,C22)	-20.3	-21.1	-21.0	-20.1
(C8,C20,C21,C54)	127.7	127.3	127.3	127.9
(C56,C20,C21,C22)	-136.2	-136.1	-136.1	-136.2
(C56,C20,C21,C54)	11.9	12.4	12.2	11.8
(Cl65,C20,C21,C22	103.4	102.9	103.1	103.6
(Cl65,C20,C21,C54	-108.5	-108.7	-108.7	-108.4
(C8,C20,C56,C55)	-127.9	-127.5	-127.5	-128.1
(C8,C20,C56,C57)	22.8	23.6	23.4	22.5
(C21,C20,C56,C55)	-12.4	-13.0	-12.7	-12.4
(C21,C20,C56,C57)	138.2	138.0	138.1	138.3
(Cl65,C20,C56,C55	108.6	108.8	108.8	108.5
(Cl65,C20,C56,C57	-100.8	-100.1	-100.3	-100.9
(C20,C21,C22,C19)	-1.6	-1.4	-1.6	-1.6
(C20,C21,C22,C23)	144.4	144.8	144.7	144.3
(C54,C21,C22,C19)	-146.3	-146.6	-146.5	-146.2
(C54,C21,C22,C23)	-0.3	-0.4	-0.3	-0.3
(C20,C21,C54,C53)	-151.8	-152.1	-152.0	-151.8
(C20,C21,C54,C55)	-7.3	-7.6	-7.5	-7.2
(C22,C21,C54,C53)	-3.0	-2.8	-3.0	-3.0
(C22,C21,C54,C55)	141.5	141.6	141.5	141.5
(C19,C22,C23,C24)	9.3	9.6	9.5	9.2
(C19,C22,C23,C52)	153.6	153.8	153.9	153.6
(C21,C22,C23,C24)	-141.0	-140.9	-141.1	-141.0
(C21,C22,C23,C52)	3.3	3.3	3.3	3.4
(C22,C23,C24,C18)	0.4	0.5	0.5	0.5
(C22,C23,C24,C25)	146.2	146.1	146.2	146.2
(C52,C23,C24,C18)	-144.6	-144.4	-144.6	-144.6
(C52,C23,C24,C25)	1.1	1.1	1.1	1.1
(C22,C23,C52,C51)	-140.5	-140.4	-140.4	-140.4
(C22,C23,C52,C53)	-3.1	-3.0	-3.1	-3.1
(C24,C23,C52,C51)	0.1	0.0	0.2	0.2
(C24,C23,C52,C53)	137.5	137.5	137.5	137.5
(C18,C24,C25,C26)	2.6	2.3	2.5	2.6
(C18,C24,C25,C50)	139.8	139.6	139.6	139.7
(C23,C24,C25,C26)	-138.8	-138.8	-138.8	-138.8
(C23,C24,C25,C50)	-1.6	-1.5	-1.7	-1.7
(C24,C25,C26,C16)	0.4	0.5	0.4	0.4
(C24,C25,C26,C27)	142.2	142.3	142.1	142.1
(C50,C25,C26,C16)	-141.5	-141.5	-141.5	-141.5
(C50,C25,C26,C27)	0.3	0.3	0.3	0.2
(C24,C25,C50,C49)	-141.4	-141.6	-141.4	-141.4
(C24,C25,C50,C51)	0.8	0.8	0.9	0.9
(C26,C25,C50,C49)	-0.1	-0.1	-0.1	-0.1
(C26,C25,C50,C51)	142.2	142.2	142.2	142.2
(C16,C26,C27,C28)	-1.5	-1.5	-1.5	-1.6
(C16,C26,C27,C49)	141.0	141.0	141.0	141.0
(C25,C26,C27,C28)	-142.8	-142.8	-142.8	-142.8
(C25,C26,C27,C49)	-0.3	-0.3	-0.3	-0.3
(C26,C27,C28,C14)	0.0	0.0	0.0	0.0
(C26,C27,C28,C38)	137.9	137.9	137.9	138.0
(C49,C27,C28,C14)	-137.9	-137.9	-137.9	-138.0
(C49,C27,C28,C38)	0.0	0.0	0.0	0.0
(C26,C27,C49,C36)	-142.1	-142.2	-142.2	-142.2

(C26,C27,C49,C50)	0.3	0.3	0.3	0.2
(C28,C27,C49,C36)	0.3	0.2	0.3	0.3
(C28,C27,C49,C50)	142.7	142.7	142.7	142.7
(C14,C28,C38,C37)	142.1	142.2	142.2	142.2
(C14,C28,C38,C39)	-0.3	-0.3	-0.3	-0.2
(C27,C28,C38,C37)	-0.3	-0.2	-0.3	-0.3
(C27,C28,C38,C39)	-142.7	-142.7	-142.7	-142.7
(C11,C29,C58,C40)	140.5	140.4	140.4	140.4
(C11,C29,C58,C41)	3.1	3.0	3.1	3.1
(C12,C29,C58,C40)	-0.1	0.0	-0.2	-0.2
(C12,C29,C58,C41)	-137.5	-137.5	-137.5	-137.5
(C37,C30,C31,C32)	138.0	138.0	138.0	138.0
(C37,C30,C31,C40)	-0.1	-0.1	-0.1	-0.1
(C60,C30,C31,C32)	-0.1	0.0	0.0	-0.1
(C60,C30,C31,C40)	-138.1	-138.1	-138.1	-138.1
(C31,C30,C37,C36)	-142.5	-142.5	-142.5	-142.5
(C31,C30,C37,C38)	0.0	0.0	0.0	0.1
(C60,C30,C37,C36)	0.0	0.0	0.0	0.0
(C60,C30,C37,C38)	142.5	142.5	142.5	142.6
(C31,C30,C60,C34)	0.1	0.1	0.1	0.1
(C31,C30,C60,C35)	142.5	142.5	142.5	142.5
(C37,C30,C60,C34)	-142.4	-142.4	-142.4	-142.4
(C37,C30,C60,C35)	0.0	0.1	0.0	0.1
(C30,C31,C32,C33)	-0.1	-0.1	-0.1	-0.1
(C30,C31,C32,C41)	-142.7	-142.8	-142.8	-142.8
(C40,C31,C32,C33)	142.5	142.5	142.5	142.5
(C40,C31,C32,C41)	-0.1	-0.1	-0.1	-0.1
(C30,C31,C40,C39)	0.1	0.1	0.1	0.1
(C30,C31,C40,C58)	142.7	142.7	142.7	142.7
(C32,C31,C40,C39)	-142.5	-142.5	-142.5	-142.5
(C32,C31,C40,C58)	0.1	0.1	0.1	0.1
(C31,C32,C33,C34)	0.3	0.3	0.3	0.3
(C31,C32,C33,C44)	-137.6	-137.6	-137.6	-137.7
(C41,C32,C33,C34)	138.3	138.4	138.4	138.4
(C41,C32,C33,C44)	0.4	0.5	0.5	0.4
(C31,C32,C41,C42)	141.4	141.5	141.4	141.4
(C31,C32,C41,C58)	0.1	0.1	0.1	0.1
(C33,C32,C41,C42)	-1.1	-1.1	-1.2	-1.1
(C33,C32,C41,C58)	-142.5	-142.5	-142.5	-142.5
(C32,C33,C34,C46)	-142.6	-142.6	-142.6	-142.6
(C32,C33,C34,C60)	-0.2	-0.2	-0.2	-0.2
(C44,C33,C34,C46)	-0.3	-0.2	-0.3	-0.2
(C44,C33,C34,C60)	142.1	142.1	142.1	142.2
(C32,C33,C44,C43)	1.0	1.0	1.1	1.1
(C32,C33,C44,C45)	142.7	142.7	142.7	142.7
(C34,C33,C44,C43)	-141.5	-141.5	-141.4	-141.4
(C34,C33,C44,C45)	0.2	0.2	0.2	0.1
(C33,C34,C46,C45)	0.3	0.2	0.3	0.2
(C33,C34,C46,C47)	142.6	142.6	142.6	142.6
(C60,C34,C46,C45)	-142.1	-142.1	-142.1	-142.2
(C60,C34,C46,C47)	0.2	0.2	0.2	0.2
(C33,C34,C60,C30)	0.0	0.1	0.0	0.1
(C33,C34,C60,C35)	-138.0	-138.0	-138.0	-138.0
(C46,C34,C60,C30)	138.0	138.0	138.0	138.0
(C46,C34,C60,C35)	0.0	-0.1	0.0	-0.1
(C48,C35,C36,C37)	142.5	142.5	142.5	142.5
(C48,C35,C36,C49)	0.0	0.0	0.0	-0.1
(C60,C35,C36,C37)	0.0	0.0	0.0	0.0
(C60,C35,C36,C49)	-142.5	-142.5	-142.5	-142.6

(C36,C35,C48,C47)	-138.0	-138.0	-138.0	-138.0
(C36,C35,C48,C51)	0.1	0.1	0.1	0.1
(C60,C35,C48,C47)	0.1	0.0	0.0	0.1
(C60,C35,C48,C51)	138.1	138.1	138.1	138.1
(C36,C35,C60,C30)	0.0	-0.1	0.0	-0.1
(C36,C35,C60,C34)	142.4	142.4	142.4	142.4
(C48,C35,C60,C30)	-142.5	-142.5	-142.5	-142.5
(C48,C35,C60,C34)	-0.1	-0.1	-0.1	-0.1
(C35,C36,C37,C30)	0.0	0.0	0.0	0.0
(C35,C36,C37,C38)	-142.5	-142.4	-142.5	-142.5
(C49,C36,C37,C30)	142.5	142.4	142.5	142.5
(C49,C36,C37,C38)	0.0	0.0	0.0	0.0
(C35,C36,C49,C27)	137.8	137.8	137.8	137.8
(C35,C36,C49,C50)	0.0	-0.1	0.0	0.0
(C37,C36,C49,C27)	-0.3	-0.2	-0.3	-0.3
(C37,C36,C49,C50)	-138.1	-138.1	-138.2	-138.2
(C30,C37,C38,C28)	-137.8	-137.8	-137.8	-137.8
(C30,C37,C38,C39)	0.0	0.1	0.0	0.0
(C36,C37,C38,C28)	0.3	0.2	0.3	0.3
(C36,C37,C38,C39)	138.1	138.1	138.2	138.2
(C28,C38,C39,C13)	0.1	0.1	0.1	0.1
(C28,C38,C39,C40)	142.2	142.2	142.2	142.2
(C37,C38,C39,C13)	-142.2	-142.2	-142.2	-142.2
(C37,C38,C39,C40)	0.0	-0.1	-0.1	-0.1
(C13,C39,C40,C31)	137.7	137.7	137.7	137.7
(C13,C39,C40,C58)	-0.4	-0.4	-0.4	-0.4
(C38,C39,C40,C31)	0.0	0.0	0.0	0.0
(C38,C39,C40,C58)	-138.2	-138.2	-138.2	-138.2
(C31,C40,C58,C29)	-141.6	-141.7	-141.6	-141.6
(C31,C40,C58,C41)	0.0	-0.1	-0.1	-0.1
(C39,C40,C58,C29)	0.9	0.8	1.0	1.0
(C39,C40,C58,C41)	142.5	142.4	142.5	142.5
(C32,C41,C42,C43)	0.3	0.3	0.4	0.3
(C32,C41,C42,C59)	-140.5	-140.5	-140.5	-140.5
(C58,C41,C42,C43)	137.6	137.7	137.6	137.6
(C58,C41,C42,C59)	-3.2	-3.1	-3.2	-3.2
(C32,C41,C58,C29)	142.0	142.1	142.0	142.0
(C32,C41,C58,C40)	0.0	0.0	0.0	0.0
(C42,C41,C58,C29)	0.2	0.2	0.2	0.2
(C42,C41,C58,C40)	-141.9	-141.9	-141.8	-141.8
(C41,C42,C43,C44)	1.2	1.2	1.2	1.2
(C41,C42,C43,C57)	-144.2	-144.1	-144.3	-144.2
(C59,C42,C43,C44)	146.3	146.2	146.3	146.3
(C59,C42,C43,C57)	0.9	1.0	0.9	0.9
(C41,C42,C59,C10)	151.8	152.1	152.0	151.8
(C41,C42,C59,C11)	3.0	2.8	3.0	3.0
(C43,C42,C59,C10)	7.3	7.6	7.5	7.2
(C43,C42,C59,C11)	-141.5	-141.6	-141.5	-141.5
(C42,C43,C44,C33)	-1.8	-1.8	-1.9	-1.9
(C42,C43,C44,C45)	-139.3	-139.3	-139.3	-139.3
(C57,C43,C44,C33)	139.4	139.3	139.3	139.3
(C57,C43,C44,C45)	1.9	1.8	1.9	1.9
(C42,C43,C57,C10)	-8.7	-9.2	-9.0	-8.7
(C42,C43,C57,C56)	143.3	143.3	143.3	143.3
(C44,C43,C57,C10)	-153.9	-154.3	-154.1	-153.9
(C44,C43,C57,C56)	-1.9	-1.8	-1.9	-1.9
(C33,C44,C45,C46)	0.0	0.0	0.0	0.0
(C33,C44,C45,C55)	-142.0	-142.0	-141.9	-141.9
(C43,C44,C45,C46)	142.0	142.0	141.9	141.9

(C43,C44,C45,C55)	0.0	0.0	0.0	0.0
(C44,C45,C46,C34)	-0.2	-0.2	-0.2	-0.1
(C44,C45,C46,C47)	-142.7	-142.7	-142.7	-142.7
(C55,C45,C46,C34)	141.5	141.5	141.4	141.4
(C55,C45,C46,C47)	-1.0	-1.0	-1.1	-1.1
(C44,C45,C55,C54)	139.3	139.3	139.3	139.3
(C44,C45,C55,C56)	-1.9	-1.8	-1.9	-1.9
(C46,C45,C55,C54)	1.8	1.8	1.9	1.9
(C46,C45,C55,C56)	-139.4	-139.3	-139.3	-139.3
(C34,C46,C47,C48)	-0.3	-0.3	-0.3	-0.3
(C34,C46,C47,C53)	-138.3	-138.4	-138.4	-138.4
(C45,C46,C47,C48)	137.6	137.6	137.6	137.7
(C45,C46,C47,C53)	-0.4	-0.5	-0.5	-0.4
(C46,C47,C48,C35)	0.1	0.1	0.1	0.1
(C46,C47,C48,C51)	-142.5	-142.5	-142.5	-142.5
(C53,C47,C48,C35)	142.7	142.8	142.8	142.8
(C53,C47,C48,C51)	0.1	0.1	0.1	0.1
(C46,C47,C53,C52)	142.5	142.5	142.5	142.5
(C46,C47,C53,C54)	1.1	1.1	1.2	1.1
(C48,C47,C53,C52)	-0.1	-0.1	-0.1	-0.1
(C48,C47,C53,C54)	-141.4	-141.5	-141.4	-141.4
(C35,C48,C51,C50)	-0.1	-0.1	-0.1	-0.1
(C35,C48,C51,C52)	-142.7	-142.7	-142.7	-142.7
(C47,C48,C51,C50)	142.5	142.5	142.5	142.5
(C47,C48,C51,C52)	-0.1	-0.1	-0.1	-0.1
(C27,C49,C50,C25)	-0.1	-0.1	-0.1	-0.1
(C27,C49,C50,C51)	-142.2	-142.2	-142.2	-142.2
(C36,C49,C50,C25)	142.2	142.2	142.2	142.2
(C36,C49,C50,C51)	0.0	0.1	0.1	0.1
(C25,C50,C51,C48)	-137.7	-137.7	-137.7	-137.7
(C25,C50,C51,C52)	0.4	0.4	0.4	0.4
(C49,C50,C51,C48)	0.0	0.0	0.0	0.0
(C49,C50,C51,C52)	138.2	138.2	138.2	138.2
(C48,C51,C52,C23)	141.6	141.7	141.6	141.6
(C48,C51,C52,C53)	0.0	0.1	0.1	0.1
(C50,C51,C52,C23)	-0.9	-0.8	-1.0	-1.0
(C50,C51,C52,C53)	-142.5	-142.4	-142.5	-142.5
(C23,C52,C53,C47)	-142.0	-142.1	-142.0	-142.0
(C23,C52,C53,C54)	-0.2	-0.2	-0.2	-0.2
(C51,C52,C53,C47)	0.0	0.0	0.0	0.0
(C51,C52,C53,C54)	141.9	141.9	141.8	141.8
(C47,C53,C54,C21)	140.5	140.5	140.5	140.5
(C47,C53,C54,C55)	-0.3	-0.3	-0.4	-0.3
(C52,C53,C54,C21)	3.2	3.1	3.2	3.2
(C52,C53,C54,C55)	-137.6	-137.7	-137.6	-137.6
(C21,C54,C55,C45)	-146.3	-146.2	-146.3	-146.3
(C21,C54,C55,C56)	-0.9	-1.0	-0.9	-0.9
(C53,C54,C55,C45)	-1.2	-1.2	-1.2	-1.2
(C53,C54,C55,C56)	144.2	144.1	144.3	144.2
(C45,C55,C56,C20)	153.9	154.3	154.1	153.9
(C45,C55,C56,C57)	1.9	1.8	1.9	1.9

Table S3. The calculated at four different levels and experimental ^{13}C NMR isotropic chemical shifts (in tetrachloromethane with deuteriated chloroform solvent, ppm) of $C_{60}Cl_6$ molecule

Cal. chemical shifts (ppm) (in tetrachloromethane with deuteriated chloroform)					Exp.*	Cal.chemical shifts (ppm) (in gas)			
Nucleus Carbon	B3LYP/6-31G(d,p)	RM062X/6-31G(d,p)	HSEH1PBE/6-31G(d,p),	B3LYP/6-311++G(d,p)		B3LYP/6-31G(d,p)	RM062X/6-31G(d,p)	HSEH1PBE/6-31G(d,p),	B3LYP/6-311++G(d,p)
C2	150.1	164.4	145.7	169.8	152.8	150.0	164.1	145.5	169.7
C7	150.1	164.4	145.7	169.8	151.0	150.0	164.1	145.5	169.7
C11	146.8	160.7	142.6	166.2	148.3	146.8	160.7	142.5	166.2
C22	146.8	160.7	142.6	166.2	148.2	146.8	160.7	142.5	166.2
C36	143.2	156.9	138.6	162.6	147.6	142.8	156.5	138.5	161.9
C37	143.2	156.9	138.6	162.6	147.6	142.8	156.5	138.5	161.9
C30	143.0	156.8	138.5	161.5	147.6	142.5	156.2	137.9	161.5
C35	143.0	156.8	138.5	161.5	147.6	142.5	156.2	137.9	161.5
C5	142.9	156.6	138.4	161.4	147.2	142.3	156.1	137.8	161.1
C17	142.9	156.5	138.4	161.4	147.1	142.3	156.1	137.8	161.1
C60	142.4	156.5	137.9	161.3	146.9	142.2	156.0	137.7	160.7
C32	142.3	156.3	137.9	161.3	146.5	142.2	155.6	137.7	160.7
C47	142.3	156.3	137.7	161.0	146.4	141.8	155.6	137.1	160.3
C21	142.2	156.2	137.7	161.0	146.4	141.6	155.6	137.0	160.3
C59	142.2	156.2	137.7	161.0	146.2	141.6	155.6	137.0	160.3
C33	142.2	156.2	137.7	161.0	144.2	141.6	155.6	137.0	160.3
C46	142.2	156.2	137.7	160.9	144.0	141.6	155.6	137.0	160.2
C27	142.2	155.7	137.5	160.9	143.5	141.5	155.5	136.9	160.2
C28	142.2	155.7	137.5	160.3	143.2	141.5	155.5	136.9	159.6
C40	141.5	155.6	136.8	160.3	142.8	140.8	155.0	136.2	159.6
C51	141.5	155.6	136.8	160.2	142.3	140.8	155.0	136.2	159.5
C38	141.1	155.3	136.1	160.2	142.0	140.5	154.7	135.5	159.5
C49	141.1	155.3	136.1	159.5	141.8	140.5	154.7	135.5	158.9
C34	141.1	155.3	136.1	159.5	141.6	140.4	154.7	135.5	158.9
C31	140.9	155.3	136.1	159.1	140.8	140.3	154.7	135.5	158.4
C48	140.9	155.2	136.1	159.1	140.5	140.3	154.6	135.5	158.4
C39	140.8	155.1	136.0	158.6	140.2	140.2	154.5	135.4	157.9
C50	140.8	155.1	136.0	157.7		140.2	154.5	135.4	157.0
C44	138.1	152.2	133.7	157.4		137.4	151.5	133.1	156.7
C45	138.1	152.2	133.7	157.4		137.4	151.5	133.1	156.7
C14	138.0	152.0	133.4	157.0		137.3	151.3	132.7	156.3
C26	138.0	152.0	133.4	157.0		137.3	151.3	132.7	156.3

C8	137.8	151.7	133.4	156.4		137.1	151.1	132.7	155.8
C9	137.8	151.7	133.4	156.4		137.1	151.1	132.7	155.8
C41	137.3	151.5	132.7	156.3		136.7	151.0	132.3	155.6
C53	137.3	151.5	132.7	156.3		136.7	151.0	132.3	155.6
C43	137.1	151.2	132.6	156.0		136.7	150.6	132.0	155.5
C55	137.1	151.2	132.6	156.0		136.7	150.6	132.0	155.5
C52	136.9	150.6	132.2	155.9		136.3	150.2	131.8	155.3
C58	136.9	150.6	132.2	155.9		136.3	150.2	131.8	155.3
C12	136.6	150.6	132.1	155.3		136.2	150.2	131.5	155.0
C24	136.6	150.6	132.1	155.3		136.2	150.2	131.5	155.0
C15	136.2	150.6	131.9	154.3		135.9	150.2	131.5	153.9
C16	136.2	150.6	131.9	154.3		135.9	150.2	131.5	153.9
C13	136.0	150.2	131.3	154.1		135.4	149.6	130.7	153.6
C25	136.0	150.2	131.3	154.1		135.4	149.6	130.7	153.6
C23	135.5	149.5	131.0	153.9	135.4	135.2	148.9	130.6	153.4
C29	135.5	149.5	131.0	153.9		135.2	148.9	130.6	153.4
C42	134.4	149.3	130.0	153.3		134.5	148.7	130.0	153.4
C54	134.4	149.3	130.0	153.3		134.5	148.7	130.0	153.4
C56	134.4	148.2	129.9	152.7		134.1	148.3	129.5	152.4
C57	134.4	148.2	129.9	152.7		134.1	148.3	129.5	152.4
C4	129.2	143.2	124.7	147.0		129.4	143.3	124.9	147.1
C18	129.2	143.2	124.7	147.0		129.4	143.3	124.9	147.1
C1	76.5	70.8	67.8	89.4	69.4	75.8	70.2	67.2	88.9
C6	74.9	66.9	65.6	87.0	66.5	74.0	66.2	64.9	86.3
C3	63.1	55.2	54.8	75.5	55.4	62.2	54.6	54.1	74.7
C19	63.1	55.2	54.8	75.5		62.2	54.6	54.1	74.7
C10	62.2	54.5	53.9	74.6		61.4	53.9	53.2	73.8
C20	62.2	54.5	53.9	74.6	54.9	61.4	53.9	53.2	73.8

*Taken from ref. [49].